Quantifiable effectiveness of experimental scaling of river- and delta morphodynamics and stratigraphy

M.G. Kleinhans, W.M. van Dijk, W.I. van de Lageweg
D.C.J.D Hoyal, H. Markies, M. van Maarseveen, C. Roosendaal
W. van Weesep, D. van Breemen, R. Hoendervoogt and N. Cheshier

Faculty of Geosciences, Department of Physical Geography, Utrecht University, Utrecht, The Netherlands.
ExxonMobil Upstream Research, Houston, USA
woutvandijk@gmail.com

Abstract

Laboratory experiments to simulate landscapes and stratigraphy often suffer from scale effects, because reducing length- and time scales leads to different behaviour of water and sediment. Classically, scaling proceeded from dimensional analysis of the equations of motion and sediment transport, and minor concessions, such as vertical length scale distortion, led to acceptable results. In the past decade many experiments were done that seriously violated these scaling rules, but nevertheless produced significant and insightful results that resemble the real world in quantifiable ways. Here we focus on self-formed fluvial channels and channel patterns in experiments. The objectives of this paper are 1) to identify what aspects of scaling considerations are most important for experiments that simulate morphodynamics and stratigraphy of rivers and deltas, 2) to establish a design strategy for experiments based on a combination of relaxed classical scale rules, theory of bars and meanders, and small-scale experiments focussed at specific processes. We present a number of small laboratory setups and protocols that we use to rapidly quantify erosive and sedimentary types of forms and dynamics that develop in the landscape experiments as a function of detailed properties such as effective material strength and to assess potential scale effects. Most importantly, the width-to-depth ratio of channels determines the bar pattern and meandering tendency. The strength of floodplain material determines these channel dimensions, and theory predicts that laboratory rivers should have 1.5 times larger width-to-depth ratios for the same bar pattern. We show how floodplain formation can be controlled by adding silt-sized silica flour, bentonite, Medicago sativa (alfalfa) or Partially Hydrolyzed PolyAcrylamide (a synthetic polymer) to poorly sorted sediment. The experiments demonstrate that there is a narrow range of conditions between no mobility of bed or banks, and too much mobility. The density of vegetation and the volume proportion of silt allow well-controllable channel dimensions whereas the polymer proved difficult to control. The theory, detailed methods of quantification and experimental setups presented here show that the rivers and deltas created in the laboratory seem to behave as natural rivers when the experimental conditions adhere to the relaxed scaling rules identified herein, and that required types of fluvio-deltaic morphodynamics can be provoked by conditions and sediments selected on the basis of a series of small-scale experiments.

1. INTRODUCTION

Experiments to simulate landscapes and stratigraphy at the laboratory scale have been used for more than a century (Reynolds, 1887). Experiments have two advantages over real-world data, namely full control over the initial and boundary conditions, and rapid evolution that can be witnessed and recorded. Experiments also have advantages over numerical modelling, namely materiality: the materials and processes at work in the experiment are real as in the natural world, unlike those in numerical models that are virtual (Paola et al., 1992; Morgan, 2003; Kleinhans et al., 2005). Such models, even if based on the laws of physics, remain dependent on choices about the included physics, specification of boundary conditions and resolution, and numerical issues related to discretisation and propagation of errors (Oreskes et al., 1994; Kleinhans et al., 2005).

A disadvantage of landscape experiments is that the length- and time-scales cannot be scaled down perfectly. Typically, scale problems of replication of the prototype, i.e. the natural system that is targeted in the experiment, increase with decreasing scales of experiments (Yalin, 1971; Schumm et al., 1987; Peakall et al., 1996). Some scale problems increase gradually, such as vertical distortion of dimensions and reduction of sediment mobility. Other scale problems appear suddenly when certain thresholds are crossed at which the character of flow and sediment transport changes dramatically. The gravest scale problems are expected in analogue models but even these problems may be acceptable depending on application (Schumm et al., 1987; Paola et al., 2009). Often such analogue models are applied in the context of stratigraphy. Depositional architecture is caused by the dynamics of morphology, including sedimentary and erosional processes associated with channel migration and scouring. Hence, the key issue for experimental studies of stratigraphy is to

reproduce the relevant morphodynamics (Paola and Borgman, 1991; van de Lageweg et al., 2013a).
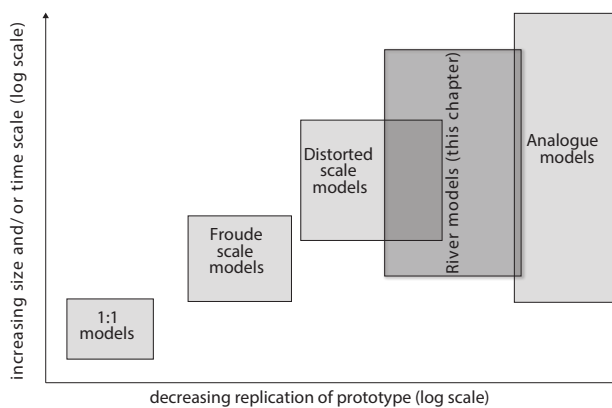
Figure 1: *Schematic view (after Peakall et al., 1996) of the balance between scales and scale problems in replicating prototypes, i.e. the natural system that is targeted. Here we address river models at a scale between distorted scale models and analogue models.*

This paper addresses scale effects for self-formed rivers and deltas with erodible banks at equal and smaller scales than distorted scale models and equal and larger scales than analogue models (Fig. 1). Traditionally, rivers with fixed banks were down-scaled to the laboratory through dynamic similarity of flow and sediment mobility expressed in dimensionless numbers (Reynolds, 1887; Yalin, 1971; Schumm et al., 1987; de Vries et al., 1990; Hughes, 1993). Similarity scaling has been a powerful measurement-, analysis- and prediction tool for scientific study and engineering. The strong emphasis on the scale rules was justified for these purposes, particularly some decades ago when numerical models and computer power were limited. However, rigidity in the adherence to scale rules has also impeded scientific progress on experiments meant to replicate processes at large spatial and temporal scales in small laboratory facilities (Paola et al., 2009). Yet spectacular results replicating patterns and dynamics found in natural systems have been obtained in experimental setups that violate classical scaling rules (e.g. Schumm and Khan, 1972; Tal and Paola, 2007; Malverti et al., 2008; Kraal et al., 2008; Braudrick et al., 2009; Hoyal and Sheets, 2009; Van Dijk et al., 2012).

But how can we be reasonably certain that these experimental results represent nature when the scale rules are violated? One approach has been not to "care that specialists in sediment transport have declared that the movable-bed scale models are wrong; so, just like the bumblebee who goes on flying even though it has been declared aerodynamically impossible for him to do so, [we] keep using the movable-bed scale model, and most of the time with great success." (Le Méhauté, in Hughes, 1993, p. 245). Indeed, several authors have discussed how well small-

scale experiments reproduce spatial patterns and dynamics of natural systems (Paola et al., 2009), even if the flow is fully laminar (Malverti et al., 2008) or hydraulically smooth, which suggests that flow turbulence is of limited importance for morphological pattern formation. Progressing from such successes, Paola et al. (2009) review and propose various fruitful ways of studying and quantifying similarity between experimental and natural systems.

The fundamental problem we address here is that similarity scaling has worked well for rivers with fixed banks and for braided gravel-bed rivers (e.g. Ashworth et al., 2004), but cannot straightforwardly be applied when characteristic (e.g. bankfull) width is a dependent parameter in self-formed channels. The reason is that no convenient theory is available to scale bank erosion rate and floodplain sedimentation, because this scaling involves many more processes than flow and sediment transport in channels and on bars. Yet the balance of bank erosion and floodplain sedimentation determines channel width and channel pattern (Ferguson, 1987; Eaton and Giles, 2009; Kleinhans, 2010). As a result, experimental design of self-formed rivers and deltas is usually based on many trials and costly errors, many of which may not yield interesting results.

The first objective of this paper is to identify what aspects of scaling considerations are most important for experiments that simulate morphodynamics and stratigraphy of entire rivers and deltas. This will lead to insight into which traditional scaling rules must be adhered to in order to produce the phenomenon of interest and which rules can be relaxed. Furthermore, we will test to what extent bar theory can be used to predict bar dimensions and the transverse bed slope in curved channels to quantify the link between morphodynamics and the resulting stratigraphy. The second objective is to present a set of simple, small and fast experiments that isolate landscape-scale processes of floodplain sedimentation, bank erosion and bank failure at small scales so that the process dynamics are accelerated. We use these experiments to constrain the conditions and materials most likely to work well for replicating landscape-scale processes experimentally and compare these conditions and materials to those used in other reported experiments. The emerging strategy to combine relaxed classical scale rules, theory of bars and meanders, and small-scale experiments focussed at specific processes can be used to design landscape experiments with dynamic rivers and deltas that create stratigraphy in the process.

2. Similarity scaling, scale effects and design

The ultimate aim of river and delta experiments is to reproduce the morphology and stratigraphy of natural systems under controlled conditions. To reproduce a natural system in the laboratory, the spatial scale must be reduced. The scale ratio relates the scale N of parameter X of a river or delta in nature to the experimental river or delta:

$$N_X = \frac{X_n}{X_e} \qquad (1)$$

where subscripts n and e refer to nature (or prototype) and experiment (or scale experiment). We refer to 'large scale number (N_X)' and 'small scale' as synonymous. Geometric similarity means that all scales with dimensions of length x, y, z are equal: $N_x = N_y = N_z$, whilst distorted scale models are vertically exaggerated. Dynamic similarity entails geometric similarity and kinematic similarity, so that the ratios of all vectorial forces are the same (Hughes, 1993). This requirement cannot be fulfilled as reviewed below, so that perfect similitude is never obtained. However, similarity is possible to some extent if similitude is obtained for the most important forces whilst the requirements are relaxed for the less important.

These compromises may lead to more severe scale problems in smaller scale experiments (Fig. 1). Obviously, sediment may still be entrained, move, and be deposited to produce morphodynamics and stratigraphy on a small scale in experiments, but with large scale numbers several thresholds are crossed at which the character of flow and sediment transport changes dramatically. These we discuss below. Table 1 summarises conditions for experiments reported in literature and reports dimensional and dimensionless characteristics described in this section.

2.1. Scaling of flow, sediment transport, morphology and stratigraphy

2.1.1 Hydraulic similarity

Similarity of free surface flow requires that the ratio of inertial and gravitational forces is similar in nature and experiment. This ratio is the Froude number:

$$Fr = \frac{u}{\sqrt{gh}} \qquad (2)$$

where u = depth-averaged flow velocity, h = water depth and g = gravitational acceleration. In nature, backwater effects are important in rivers and deltas and occur only in subcritical flow. Many systems in nature have a tendency to remain subcritical (Parker, 1978; Grant, 1997; Giménez et al., 2004). Flow in ex-

periments is not necessarily subcritical with $Fr < 1$, as many experiments have localised antidunes with $Fr \geq 1$ and an average Froude number for the experiment only just below critical. Some delta experiments of Hoyal and Sheets (2009) even had supercritical flow. A simple advantage of subcritical flow is that the experimental water levels can be controlled by the downstream weir over a length similar to the e-folded backwater adaptation length in subcritical flow (i.e. the characteristic length scale over which a water level curve with exponential shape approaches the asymptote of steady uniform flow depth). This backwater adaptation length (Ribberink and Van der Sande, 1985; Parker, 2004) is estimated as:

$$\lambda_{bw} = \frac{3h}{S} \qquad (3)$$

with S = energy slope.

Scaling of flow velocity, fluid vorticity and the adaptation of spiral flow in bends requires that the flow resistance scale N_C adheres to the roughness condition (Struiksma, 1986):

$$N_C^2 = \frac{N_{x,y}}{N_z} \qquad (4)$$

However, relative to water depth both sediment particles and laboratory dunes are typically larger than dunes in real rivers. The effect of relatively larger flow resistance in experiments, with $N_C > 1$, is a lower flow velocity than required for other scaling conditions. The classical way of resolving this is by vertical distortion, which implies an exaggeration of the water depth. In small-scale channel pattern and delta experiments bedforms are generally absent or negligible so that flow is entirely determined by skin friction and energy slope.

Another requirement of similarity holds for the ratio of inertial to viscous forces as expressed in the Reynolds number:

$$Re = \frac{uh}{\nu} \qquad (5)$$

where ν = dynamic viscosity ($\nu \approx 1 \times 10^{-6}$ for water of 20°C). In natural rivers, flow is usually turbulent with a Reynolds number $Re > 2000$. The Froude and Reynolds conditions cannot be reconciled simultaneously, but the Reynolds similarity condition can be relaxed as long as flow is turbulent, that is, dominated by inertial forces, and details of turbulence are not important (e.g. Hughes, 1993).

For large length scale numbers N_X, surface tension at the interface of air, water and a solid object or boundary may become important. The relative importance of inertial and surface tension forces is

expressed in the Weber number:

$$We = \frac{\rho u^2 h}{\sigma} \qquad (6)$$

where σ = surface tensile force per unit length (0.073 N/m for pure water), where as a rule of thumb surface tension is negligible for $We > 10$ (Peakall et al., 1996). Surface tension can be modified by surfactants. Polymers in the flow may increase the surface tension, while soap may decrease it (de Gennes et al., 2004). Experimentation and analysis on the effect of soap on shallow flow and sediment transport are clearly needed before practical application becomes feasible. However, a rule of thumb for surface tension effects based on a simple threshold Weber number gives neither the effects on general flow nor the spatial extent. Theory for thin liquid films and capillarity may elucidate potential scale effects of surface tension. It is particularly instructive to assess the length scale over which surface tension may modify the flow conditions. The exponential decay of water surface perturbations caused by objects that protrude out of the flow is characterized by the capillary length λ_c. This e-folded adaptation length is found by comparing the Laplace pressure σ/λ_c with the hydrostatic pressure $\rho g h$ (de Gennes et al., 2004), where:

$$\lambda_c = \sqrt{\frac{\sigma}{\rho g}} \qquad (7)$$

For water this yields a capillary length $\lambda_c = 2.7$ mm. Hence the hydraulics are significantly modified by surface tension if the water depth is of the same order as the capillary length *and* if sudden bed jumps or objects such as large particles or vegetation stems are present. A more thorough analysis is presented in Malverti et al. (2008). For practical purposes we can infer from this analysis that surface tension is only important at water depths of a few mm where the largest particles protrude out of the flow or emergent plants are used, and that even then the effect is limited to enhanced sedimentation of fines within a few mm around such emergent objects, similar to tail bars behind trees or other obstructions in nature.

The near-bed flow conditions affect bed scouring tendency. The channel bed is hydraulically smooth when the particles are submerged in the laminar sublayer. When this is the case, ripples form if there is enough water depth ($h > 0.02$ m, van den Berg and van Gelder, 1993), or scour holes form in shallow flow. A full explanation for these phenomena is lacking but a reasonable working hypothesis is that the turbulence generated at the ripple crest or scour hole rim is strong enough to penetrate the laminar sublayer, so that scour is maintained. For hydraulically rough boundaries, the bed remains planar or dunes form (Kleinhans, 2005b,a). The balance between inertial and viscous forces at the bed surface is given

by the Reynolds particle number:

$$Re* = \frac{u * D_{50}}{\nu} \qquad (8)$$

where $u* = \sqrt{\tau/\rho}$ is the shear velocity. The transition from hydraulically smooth to rough conditions is gradual ($Re* = 3.5 - 70$), so that a hard threshold cannot be identified. Conservative estimates take the upper limit, but empirical evidence suggests that the limit below which scour holes and ripples form is an order of magnitude less than $Re* = 70$. Comparison to empirical bedform stability diagrams (Southard and Boguchwal, 1990; van den Berg and van Gelder, 1993) shows that the transition takes place in the lowest part of the Shields curve (Wiberg and Smith, 1987; Zanke, 2003; Vollmer and Kleinhans, 2007) at $Re* \approx 5$ (Kleinhans, 2005b,a).

2.1.2 Sediment transport similarity

The key issue in reproducing mobile bed morphology and consequent stratigraphy is sediment mobility. In nature, sand bed rivers have high mobility whereas gravel bed rivers have low mobility near the threshold for sediment motion. Sediment mobility is expressed in the form of the Shields number (θ), which is the balance between the bed shear stress and gravity:

$$\theta = \frac{\tau}{(\rho_s - \rho_f)gD} \qquad (9)$$

where in steady uniform flow $\tau = \rho_f g h S$ is the total shear stress, with ρ_f = density of fluid, ρ_s = density of sediment and D = particle diameter, usually the mean or median of the distribution by weight. For sediment transport calculations, the shear stress related to skin friction is used to exclude form roughness from bedforms and channel walls:

$$\tau = \rho_f g \frac{u^2}{C'^2} \qquad (10)$$

with the Keulegan (1938) equation to estimate the skin friction-related Chézy number (C', unit m$^{1/2}$/s van Rijn, 1984):

$$C' = 18 \log \frac{12h}{D_{90}} \qquad (11)$$

where D_{90} = 90th percentile of the particle size distribution. This condition for similarity of mobility cannot be fulfilled in conjunction with the Froude similarity because one depends on u^2 and the other on u. Furthermore, particle size cannot be reduced as much as the other Cartesian dimensions of the experiment relative to the prototype in nature, because properties such as threshold mobility and cohesion of silt and clay are significantly different from that of sand and gravel (e.g. Lick and Gailani, 2004).

In practice, the above equations are used to assess

sediment mobility *a priori* based on expected flow conditions and design sediment properties. The key problem in morphological experiments is that these sediments cannot be much different from those in nature, yet the shear stress is much lower. Given the small water depth of small-scale experiments, the typical shear stress is low despite larger bed slopes than in nature. Hence sediment mobility may be low or even below the threshold of sediment motion. Three ways have classically been applied to increase sediment mobility. The first is to vertically distort the model, that is, $N_h > N_L$. This has the advantages of increasing slopes and also of decreasing surface tension effects. The second is to further increase the bed slope of the experiment, which is known as tilting. The third way is to use light-weight materials as bed sediment (Yalin, 1971; Hughes, 1993). Although very useful, light-weight sediment have been predicted to lead to subtle scale effects on bar dimensions (discussed later).

High bed slope and small water depth in experiments also affects the threshold for the initiation of sediment motion, i.e. the Shields criterion, which may therefore differ from that in nature (Vollmer and Kleinhans, 2007). This modification becomes particularly important in shallow flows where the largest particles protrude above the flow surface (Ferguson, 2007). Furthermore, steeper slopes and effects of shallow flow on different particle sizes may affect sediment sorting patterns. The mobility of size-fractions in sediment mixtures are still relatively poorly understood for small-scale experiments (Wilcock and Crowe, 2003; Vollmer and Kleinhans, 2008), but data indicate that the sediment mixture should be unimodal in order to have equal mobility of all size fractions and prevent limited mobility of the large fractions (Parker and Klingeman, 1982; Wilcock, 1993; Kleinhans and Van Rijn, 2002). Such lower mobility would result in sediment sorting patterns such as armouring. On the other hand, there are also conditions in which coarse particles become more mobile than the average grain size. In shallow experimental flows where D approaches h, coarser particles may be more prone to overpassing onto the bars than in nature because of limited water depth relative to particle size (Carling, 1990). Furthermore, in extreme cases of channel slopes of about 0.05, the relative mobility of finer and coarser sediment reverses because the bed tilt significantly changes the force balance on the large exposed particles (Solari and Parker, 2000).

The Reynolds particle number (Eq. 8) characterises an important aspect of sediment mobility in addition to the Shields number: It directly compares the size of a particle resting on the bed and the thickness of the laminar sublayer, just above the bed, in which turbulence is suppressed. Roughness and turbulence generation are also dependent on particle shape, in particular angularity, and the particle size distribution. This may be part of the reason that Stefanon et al. (2010) obtained morphology dominated by the typical scour holes associated with hydraulically smooth conditions. Their sediment was a uniform 0.8 mm polystyrene, which probably was moderately well rounded. On the other hand, Peakall et al. (2007) had hydraulically rough conditions despite the D_{50} being only 0.21 mm. The probable reason for this hydraulic behaviour is that the D_{90} is nearly 2 mm, and Peakall et al. (1996) argue that the Reynolds particle number should be calculated with the D_{90} rather than the D_{50}. Consequently, the advantage of a poorly sorted sediment is that sediment mobility, related to the median particle size, remains relatively high whilst the bed remains hydraulically rough.

Self-formed floodplain are essential elements in channel pattern (Kleinhans, 2010), and form from bedload and suspended sediment deposited in splays and levees, from clay in floodbasins and from flow resistance induced by vegetation. The degree of suspension can in principle be assessed by some form of Rouse number, which is the ratio of the settling velocity of sediment and a depth-averaged or shear velocity of the flow. However, sediment suspension requires turbulence, which is difficult to obtain in small-scale experiments where floodplain is likely laminar. Indeed, although most fluvial experiments (Friedkin, 1945; Smith, 1998; Tal and Paola, 2007; Peakall et al., 2007; Braudrick et al., 2009) and delta experiments (Hoyal and Sheets, 2009; van Dijk et al., 2009) had turbulent flow in the self-formed channels, laminar flow prevails on most of the floodplain. It is therefore hardly useful to assess proper scaling of suspension by comparing flow velocity on the floodplain to settling velocity of the sediment when suspension is impossible anyway for lack of turbulence. We hypothesise that experimental floodplain siltation by fines is more localised near the channel than in nature, because in the laminar flow on the floodplain the suspended sediment advected in from the channel will settle quickly as turbulence decays and floodplain flow transforms from turbulent to laminar conditions, unlike in many natural conditions. It is possible that light-weight sediments in experiments have a longer settling lag in addition to being more mobile so that these may deposit more distally in the floodplains (Braudrick et al., 2009) but this is still being explored.

An important question is how the experimental time is scaled. A characteristic morphological time scale can be calculated directly from the average sediment transport rate and a control volume that is eroded or deposited if experiments were scaled according to a similarity scaling procedure (Yalin, 1971; de Vries et al., 1990). This results in a characteristic time scale of, for instance, transverse bed slope

tilting in a curved channel, channel excavation, and of the formation of an entire delta. The appropriate time scale depends on the phenomena of interest, because it is the relevant spatial gradient of sediment transport that determines the rate of morphological change. So, on a transverse bed slope and at a channel cutoff or avulsion site, the appropriate transport rate is the transverse sediment transport component which depends on helical flow, transverse bed slope, sediment mobility and flow resistance (also see Eq. 20). For deltas with a certain volume that capture all supplied sediment and a feeder without bank erosion, the calculation of the morphological time scale for delta formation is straightforward. This approach has been applied to experimental deltas and alluvial fans (Kraal et al., 2008; van Dijk et al., 2012) and to deltas on Mars (Kleinhans et al., 2010b) to determine the formative time scale given a sediment transport rate estimated from upstream channel dimensions.

The entire analysis so far implicitly assumes simple stepped hydrographs or even constant discharge, which is a common assumption in empirical geomorphology, e.g. in hydraulic geometry relations, and in numerical morphodynamic modelling, where a constant discharge can be chosen that transports the same amount of sediment as the hydrograph. A key question is how varying discharge affects sediment transport processes, and, indirectly, channel and floodplain morphodynamics and the resulting stratigraphy. On the one hand the morphological response to individual floods is limited so that the morphology is the result of the varying discharge over a long period (Wolman and Miller, 1960). There is ample empirical evidence for this. Channel pattern prediction is empirically quite accurate on the basis of a single discharge, for example the mean annual flood or another hydrological statistic (Wolman and Miller, 1960; van den Berg, 1995). In a meandering river a series of floods and low flows including a 1 in 100 year flood had little effect on the morphology (Rhoads and Miller, 1991). On the other hand, single floods may cause much larger morphological changes than low discharge of a much longer duration. For example, floods in braided rivers caused significant re-organization of bars and channels(e.g. Bertoldi et al., 2009; Sambrook Smith et al., 2010; Marra et al., 2013). Furthermore a comparison between experimental meandering rivers created with constant discharge and with a stepped hydrograph shows that floodplain formation is much more extensive in the latter, not surprisingly (Van Dijk et al., 2013b). There is also empirical and experimental evidence, however, that the stratigraphy of channel deposits is hardly affected (Sambrook Smith et al., 2010; van de Lageweg et al., 2013b). One reason is that, as soon as the bankfull level is reached and the floodplain inundates, bed shear stresses hardly increase with increasing discharge. A higher discharge

is thus simply stored in the floodplain. Wide floodplains greatly reduce the in-channel morphological and stratigraphic effectiveness and impact of floods larger than bankfull (Rhoads and Miller, 1991). This means that such large floods are important for floodplain morphology and therefore indirectly for channel pattern, but are not very important for in-channel morphology and stratigraphy. Consequently, width limitations of experimental setups require careful consideration and the targeted scale of morphology and stratigraphy of an experiment sets the requirements.

Riparian vegetation clearly requires certain hydrographs. In experiments the low flows often have on average conditions below the threshold for sediment motion and are mainly applied to supply water to vegetation growing in the experimental systems (Tal and Paola, 2007; Braudrick et al., 2009; Van Dijk et al., 2013a). All morphological work is then done during the high discharge, which may be somewhat above bankfull. Welber et al. (2013) showed that large wood is captured at specific elevations in experimental rivers which means that the flood water levels relative to the developed surface elevation distribution is important for this aspect of biogeomorphological interaction. Perona et al. (2012) showed that the number of uprooted alfalfa plants during floods is related to plant age, which means that the time scale of vegetation development and the time scale of floods should be similar in order to have dynamic interaction. Clearly there is further scope for fundamental experimental work on interaction between plants and morphodynamics, but as experiments are relatively time-consuming a method to assess required experimental conditions and scaling is wanting.

2.1.3 Similarity of morphology, dynamics and stratigraphy

The ultimate aim of experiments is to reproduce and investigate natural river morphology, morphodynamics, morphological adaptation and the resulting stratification to a change in boundary condition. Unfortunately, morphological and stratigraphical similarity is not necessarily attained under conditions of geometric, hydraulic and sediment transport similarity. Wavelengths, migration rates and amplitudes of bars depend on channel width-to-depth ratio, mobility and the planimetric form of the channel including its curvature, width variations and sinuosity (Struiksma et al., 1985; Seminara and Tubino, 1989). Hence any vertical distortion of channels will modify the morphology and resulting stratigraphy.

In order to predict analytically the dependence of fluvial bar morphology on channel dimensions, flow conditions and sediment mobility in experiments, we apply the Struiksma et al. (1985) theory, which, as other theories (e.g. Seminara and Tubino, 1989), is

based on a physically-based description of the interaction between flow and a deformable sediment bed. The direction of sediment transport may differ from the direction of depth-averaged flow because of gravitational effects on moving particles on transverse and longitudinal slopes and because of spiral flow in bends. The first is often referred to as the transverse bed slope effect and the second is often referred to as bend flow. The steady bed topography in river bends can be understood as a combination of a transversely sloped bed depending on the local channel curvature and a pattern of steady alternate bars induced by upstream variations (or perturbations) in channel curvature. The superimposed bars are in some conditions expressed as deep pools on the outer bend, mirrored by high bars on the inner bend. The transverse bed slope and bar patterns are highly relevant for stratigraphy: the transverse bed slope effect effectively determines the slope of lateral accretion surfaces, whilst the deepest scours form the erosional base of the channel belt.

Struiksma et al. (1985) (also see Kleinhans and van den Berg, 2011) derived analytical predictors for bar wavelength and bar behaviour. This theory can intuitively be understood from the starting point of a perfectly straight channel with flat bed and an upstream perturbation of the bed on one side of the channel at a fixed location. Starting from this perturbation, the transverse flow adapts whilst the bed develops a transverse slope, which is the first bar forced by the perturbation. Depending on conditions, this bar excites new bars further downstream, or the perturbation is damped out. Struiksma et al. identified four characteristic length scales that describe such a situation, namely the adaptation length of transverse flow λ_w, the adaptation length of transverse bed adaptation λ_s, the wavelength of the bars L_p (m) and the damping length of the bar L_D (m). Most importantly, dimensionless bar period (or wavelength) L_p is calculated from:

$$\frac{2\pi\lambda_w}{L_p} = \frac{1}{2}\sqrt{(n+1)\frac{\lambda_w}{\lambda_s} - \left(\frac{\lambda_w}{\lambda_s}\right)^2 - \left(\frac{n-3}{2}\right)^2} \tag{12}$$

where n = the degree of nonlinearity of sediment transport versus depth-averaged flow velocity ($q_b = f(u^n)$). For a classical bed load transport predictor such as Meyer-Peter and Mueller (1948), $n \geq 3$ for high Shields numbers and increases to infinity towards the critical Shields number for sediment motion. We choose with $n = 4$ for sand-bed rivers and for gravel-bed rivers $n = 10$ (following Crosato and Mosselman, 2009) as gravel is closer to the threshold of motion so that the nonlinearity is stronger. Here, the adaptation length λ_w (m) of transverse flow is given as:

$$\lambda_w = \frac{C^2 h}{2g} \tag{13}$$

which suggests that adherence to the roughness scale (Eq. 4) is important. The adaptation length of a bed disturbance λ_s (m) is calculated as:

$$\lambda_s = \frac{h}{\pi^2}\left(\frac{W}{h}\right)^2 f(\theta) \tag{14}$$

where W is channel width (m), and where the magnitude of the transverse slope effect $f(\theta)$ is calculated from an empirical function (e.g. Koch and Flokstra, 1981; Talmon et al., 1995):

$$f(\theta) = \alpha_\theta \sqrt{\theta} \tag{15}$$

where α_θ is used for calibration.

Dimensionless damping length L_d of the bars is calculated by:

$$\frac{\lambda_w}{L_d} = \frac{1}{2}\left(\frac{\lambda_w}{\lambda_s} - \frac{n-3}{2}\right) \tag{16}$$

Thus bar theory predicts whether forced bars dampen out in less than one bar length (overdamped regime) or over longer distance so that multiple bars along the river may exist (underdamped regime) or excite (excitation regime, $L_d < 0$ m). This characteristic of bars is a function of the dimensionless Interaction Parameter (IP):

$$IP = \frac{\lambda_s}{\lambda_w} \tag{17}$$

which depends strongly on width-depth ratio, and weakly on hydraulic roughness and sediment mobility. The significance of this ratio is that it predicts whether bars can exist at all in a channel. For instance, very narrow and deep experimental channels will not develop bars.

The above shows that the key variable that needs to be controlled in experiments is the width-to-depth ratio of the channel. The above length scales, particularly the bar length but also the damping length that predicts bar behaviour, depend most strongly on channel aspect ratio W/h and also on roughness $h/D50$ and C, and sediment mobility θ. All variables may differ between experiment and nature because of vertical distortion, so that the eventual morphology differs as well (Struiksma et al., 1985; Struiksma, 1986). It is the question, however, how important those distortions are when river patterns are created in generic experiments without relation to a specific prototype.

The different regimes of the Interaction Parameter lead to the development of different river patterns (as described in Kleinhans and van den Berg, 2011). A river can be considered as single-thread, moderately braided or braided depending on the number of active channels across the river during channel-forming discharge (Egozi and Ashmore, 2008; Kleinhans and van den Berg, 2011). In order to assess

the effect of scaling, the above equations were directly applied to typical conditions in natural rivers and laboratory experiments. This shows that the curves of dimensionless damping and wavelengths as a function of the dimensionless Interaction Parameter for natural and laboratory scales are indistinguishable. This result was obtained with $n = 10$, for the laboratory river a $D_{50} = 0.5$ mm, $h = 0.01$ m, $C = 40$ m$^{1/2}$/s and $\theta = 0.1$ based on Table 1 and for the natural gravel-bed river a $D_{50} = 33$ mm, $h = 1.6$ m, $C = 28$ m$^{1/2}$/s and $\theta = 0.1$ based on Kleinhans and van den Berg (2011). The chosen numbers suggest a laboratory river that is about 100 times as small as a typical natural river with $N_h = 160$ and $N_D = 66$. The width-to-depth ratio required for a certain bar pattern can then be calculated for the laboratory and natural case using the definition of IP. This leads to the conclusion that to obtain the same bar pattern an experiment requires a width-to-depth ratio that is about 1.5 times larger than in the natural case.

The number of active channels are given by the braiding index (B_i) or the bar mode m. Crosato and Mosselman (2009) derived an analytical bar mode predictor, which provides the favourable mode according to the theory of Struiksma et al. (1985) for sand and gravel bed rivers:

$$m = \sqrt{\frac{0.17g\,(n-3)}{\sqrt{\frac{\rho_s - \rho_f}{\rho_f}}D_{50}}\frac{W^3 S}{CQ}} \quad (18)$$

where the relation between mode m and braiding index B_i is defined as

$$B_i = \frac{m-1}{2} + 1 \quad (19)$$

Metivier and Meunier (2003) and Malverti et al. (2008) analysed the effects of laminar flow on sediment transport and braiding and found that sediment transport in laminar flow can well be described by a Bagnold-type or Meyer-Peter and Mueller-type predictor, which depend on sediment mobility and the threshold for sediment motion. Furthermore, braided rivers were experimentally produced in laminar flow in agreement with linear stability theory by Devauchelle et al. (2007), which demonstrates that the existence of braiding does not depend on turbulence of the flow. However, the development of laminar spiral flow has yet to be investigated, so we do not know the effect of laminar flow on bar dimensions and transverse bed slope in experiments aimed at meandering. Furthermore, meandering requires formation of a floodplain, and if this is accomplished by deposition of fine suspended sediment then turbulence is required for suspension.

An analytical solution for the transverse bed slope, which corresponds to the slope of lateral ac-

cretion surfaces in river bar deposits, can be found for an infinitely long and gentle bend when the gravitational force on particles are balanced by the spiral flow (Struiksma et al., 1985; Talmon et al., 1995):

$$\tan\left(\frac{\delta z}{\delta y}\right) = 9\left(\frac{D}{h}\right)^{0.3}\sqrt{\theta}\frac{2}{\kappa^2}\left(1 - \frac{\sqrt{g}}{\kappa C}\right)\frac{h}{R} \quad (20)$$

where $\kappa = 0.4$ is Von Kármán's constant and $R = $ radius of curvature of the streamlines. This equation is very sensitive to the calibration parameter α_θ (Schuurman et al., 2013).

To sum up what can be learned from theory: to obtain geometrical similarity of channel morphology between a prototype and scale model, all dimensionless length scales should be equal, including the interaction parameter and the dimensionless damping and wavelength of the bars. Scale model distortion ($N_x = N_y \neq N_z$) leads to a significant scale problem, because the width-to-depth ratio appears in the length scales for bar development. It cannot be resolved by adjusting the sediment mobility, which also appears in the length scales, because mobility affects the sediment transport mode and transverse bed slope (see Eq. 20). The scale problems are also not improved when using a low density sediment because the balance between spiral flow and transverse bed slope effect is changed (Struiksma et al., 1985; Struiksma, 1986; Struiksma and Klaassen, 1986), although the low density would have no effect on the predicted bar pattern if the Shields mobility is kept the same by reduction of the gradient. The balance between spiral flow and transverse bed slope is also modified for different grain sizes if a poorly sorted sediment is used. On the other hand, scale models may have higher width-to-depth ratios than prototypes for the same bar pattern. In conclusion, there is no experimental approach that will completely overcome prevent these scale problems so the only option is to conduct experiments that are not ideally scaled and compare experimental results to natural systems, theory and numerical models.

2.1.4 Aim, design and characteristics of river and delta experiments

Our approach to experimental design and analysis as outlined above takes an intermediate position between the powerful similarity scaling of traditional engineering and the equally powerful exploratory landscape and stratigraphy experiments that violate scaling rules yet produce various forms of similarity between experiment and nature. Many experiments in sedimentology and geomorphology focus on generic questions rather than a specific prototype (Table 1), so the scale N (Eq. 1) is unknown. This means that geometric proportions in the experiments may be different from specific prototypes, for instance the length of bars relative to channel width,

the width-to-depth ratio and the backwater adaptation length compared to the bend or bar length. But as long as the processes and dynamics are the same or similar as those in nature, generic questions can be answered by comparison of the morphodynamics with control experiments at the same scale. Thus violations of similarity scaling can largely be ignored and theory can be used to design the experiments. Theory is in fact more appropriate for experimental river pattern design than empirical approaches; for example the empirically accurate stream power classification for river patterns Kleinhans and van den Berg (2011) breaks down for small rivers and experiments whereas the theory of Struiksma et al. (1985) predicts bar dimensions in our experiments rather well (Kleinhans et al., 2010a; Van Dijk et al., 2012).

From the foregoing, it follows that three 'relaxed' scaling requirements must be fulfilled for general process similarity with natural gravel-bed rivers. We call these requirements 'relaxed' relative to classical similarity scaling. First, flow must remain subcritical or critical and turbulent. Grant (1997) found that self-formed channels that tend to evolve into the supercritical regime will not exceed critical flow by much or will tend to oscillate around critical flow. Indeed, experiments often are close to critical and rarely exceed $Fr = 1$ (Table 1). Second, bed sediment must be mobile in the bedload regime to represent gravel bed rivers in nature and in the suspension regime to represent sand bed rivers in nature. The latter has proven difficult when very fine cohesive sediment is used (Smith, 1998; Hoyal and Sheets, 2009). Scale problems are largely unexplored in such conditions, if only because weakly cohesive sediment behaviour in laboratory conditions is poorly understood. Usually, however, experiments have dominant bed load transport which is typical for gravel-bed rivers (Kleinhans and van den Berg, 2011). Third, the bed must be hydraulically rough. This requirement conflicts with the requirement of sufficient sediment mobility, which also depends on particle size, and in the case of the smooth bed of Smith (1998) may have led to unrealistically deep scour holes and sharp bends. The conflict has been resolved by using a poorly sorted unimodal sediment where the coarsest particles cause the bed to be rough (Peakall et al., 2007; Van Dijk et al., 2012).

The key problem that now remains is to constrain material behaviour and conditions such that the dynamic balance between floodplain formation and bank erosion leads to the desired type of river or delta pattern. This consideration will determine the channel width-to-depth ratio, which must be in the range where the correct river pattern appears. For braiding experiments the channels must be wide and shallow so that higher-mode bars appear as in Ashmore (1991) and Tal and Paola (2010). The channel width-to-depth ratios of the Smith (1998) experiments are extraordinary small compared to natural systems because of the large cohesion of the sediment. The large depth could not have been caused by vertical distortion due to high flow resistance, because the fine sediments used in the experiments were relatively smooth, which is confirmed by the high Froude number. Early experiments demonstrated that lack of bank strength leads to runaway bank erosion and formation of braided systems (Friedkin, 1945; Schumm and Khan, 1972), whereas too much bank strength leads to unrealistically narrow and sometimes immobile channels (Smith, 1998). Therefore many studies attempted to form floodplains that were erodible by adding slightly cohesive sediment such as silica flour (Peakall et al., 2007), vegetation (Tal and Paola, 2010) or cohesionless low-density sediment that was mobile on the floodplain and trapped by vegetation (Braudrick et al., 2009). Most of these materials were selected by trial and error in time-consuming experiments. The problem addressed in the next section is how we can test such materials in advance to understand their influence on experimental conditions, thereby providing an a priori framework for achieving desired experimental outcomes.

3. EXPERIMENTS FOR TESTING EROSION AND SEDIMENTATION

To design an experiment with self-formed channels, one could apply hydraulic geometry relations. However, these relations implicitly depend on the strength of the banks and therefore indirectly on processes that form floodplain on the accreting bank (see Ferguson, 1987; Kleinhans, 2010, for reviews). Consequently, we must find a way to scale down the floodplain forming processes and the resulting ratio between strength of the banks relative to strength of the flow that determines bank erosion processes and rate (Simon et al., 2000; Simon and Collinson, 2002). The tendency of a small-scale fluvial system to form floodplains and erode banks depends to a large extent on the properties of the sediment and presence of vegetation or other substances that enhance bank strength, which we will first describe. Following material description, we present four experimental setups that test aspects of the balance of flow and bank strength: the direct shear test, a bank erosion experiment (Fig. 2a,b), a delta deposition experiment (Fig. 2c) and a stream table (Fig. 2d). Together these four setups can be used to *quickly* determine relevant properties and behaviour of materials (Table 2) in otherwise similar conditions, in contrast to expensive experiments with entire rivers and deltas in a large flume (Table 1) that take weeks or months to run.

Table 1: *Dimensional and dimensionless characteristics of selected river and delta experiments reported in literature (Friedkin, 1945; Schumm and Khan, 1972; Ashmore, 1991; Smith, 1998; Peakall et al., 2007; Braudrick et al., 2009; Tal and Paola, 2010; Van Dijk et al., 2012, 2013b; Sheets et al., 2002; Hoyal and Sheets, 2009).*

|	Friedkin	Schumm	Ashmore	Smith	Peakall	Braudrick	Tal	v Dijk 1	v Dijk 2	Sheets	Hoyal	Unit
Q	1.42	4.25	3	0.71	0.51	1.8	2	1	0.3	0.5	0.33	10^{-3} m^3/s
S	0.0075	0.02	0.015	0.015	0.008	0.0046	0.015	0.0055	0.01	0.05	NA	m/m
D_{10}	0.2	0.35	0.2	0.01	0.12	0.62	0.3	0.25	0.25	0.12	0.005	10^{-3} m
D_{50}	1.2	1.16	0.7	0.03	0.21	0.8	0.5	0.51	0.51	0.12	0.05	10^{-3} m
D_{90}	3	4	1.2	0.05	1.03	1.04	0.7	1.35	1.35	0.12	0.45	10^{-3} m
W	0.23	0.671	1.0	0.04	0.116	0.4	0.4	0.3	0.15	0.115	0.05	m
h	0.0457	0.0762	0.01	0.005	0.015	0.013	0.02	0.015	0.010	0.028	0.023	m
Fr	0.19	0.10	0.95	0.90	0.76	0.87	0.56	0.78	0.80	0.30	0.59	-
λ_{bw}	18.3	114.3	2.0	1.0	5.6	8.5	4.0	8.2	3.0	1.65	15.1	m
Re	5800	6400	3000	1000	4400	4100	5000	4500	2500	4400	6600	-
We	10.1	7.3	12.3	2.7	17.6	17.3	17.1	18.5	8.6	9.4	25.7	-
Re^*	174.0	46.4	153.4	1.4	35.3	25.2	38.0	45.9	45.9	34.8	0.16	-
θ	0.17	0.13	0.08	1.52	0.35	0.05	0.36	0.10	0.12	6.94	0.14	-
C	40.7	51.9	26.6	55.5	40.4	39.2	45.6	38.3	35.1	54.7	85.4	m$^{1/2}$/s
n	10	10	10	4	10	10	10	10	10	4	10	-
Lp	0.64	1.51	-	1.78	-	5.34	2.37	3.95	1.52	0.77	-	m
Ld	-0.38	-0.28	-0.36	0.19	0.26	11.4	-0.28	2.04	1.02	-0.38	0.014	m
IP	0.43	1.02	7.88	0.30	0.30	0.26	1.96	0.20	0.21	4.28	0.004	-
B_i	1.36	1.83	4.45	1.0	1.0	1.17	2.34	1.17	1.17	1.53	1.0	-

3.1. Materials

Three sediment mixtures used herein the range reported in literature(Fig. 3). One sediment is uniform fine sand as used in van Dijk et al. (2009). The other sediments are poorly sorted sand as in Peakall et al. (2007) and Van Dijk et al. (2012); van de Lageweg et al. (2013a). We also studied the behaviour of even more poorly sorted sediment but found that it armoured strongly so that material is not included here. Silt-sized silica flour was added to the poorly sorted sand in Fig. 3 various proportions. How this silt affects the morphodynamics is not fully understood, but it is the only granular material discovered so far that builds floodplain at the experimental scale that leads to dynamic meandering. Although the silt is not nearly as cohesive as clay, Lick and Gailani (2004) show that the critical shear stress increases for particles smaller than 50 μm, so that the added silica flour is expected to increase the threshold for channel erosion on a floodplain. At the same time, the silt particles percolate through the pores into the bed and silt smaller than a certain cutoff size does not contribute to bed level change and roughness (Frings et al., 2008). We calculated that silt-sized material finer than 20 μm, that is, 40% of the silt-sized silica

flour, is accommodated entirely in the pore space of the sand mixture, which means that more than half of the silt is deposited on top of the sand to form slightly cohesive layers with smooth surfaces.

Two materials were added to the poorly sorted sediment in some experiments: bentonite and Partially Hydrolyzed PolyAcrylamide (PHPA, a synthetic polymer). The bentonite is a clay mineral that was mixed into the sand in dry powder form. The polymer was used in the delta experiments of Hoyal and Sheets (2009) in combination with the bentonite and other materials. For an experiment with distinct channels and floodplain it is important to be able to measure where the polymer is deposited, but, unlike the other materials, PHP is difficult to observe. We unsuccessfully attempted to dye the polymer and also attempted to measure the polymer concentration with an amide hydrolysis method (Nagase and Sakaguchi, 1965). For both methods the measurable polymer concentration in a soil sample turned out to be an order of magnitude higher than the low polymer concentrations at which morphodynamics were already strongly affected. More importantly, we found from percolation experiments with coloured polymer that the polymer was not fixated in the
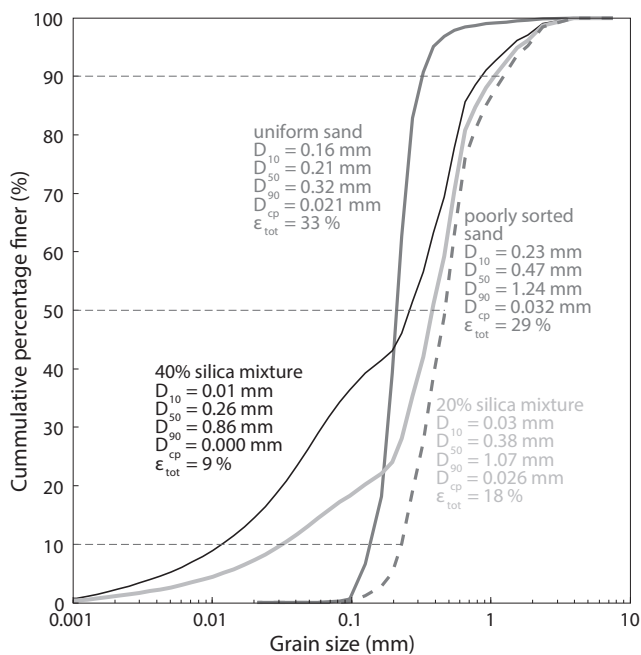
Table 2: *Approximate conditions in three small experimental setups (see Fig. 2) in comparison to the large flume experiment with self-formed river and floodplain of Van Dijk et al. (2012, 2013b); van de Lageweg et al. (2013a).*

Setup	discharge 10^{-3} m^3/s	sediment feed 10^{-3} m^3/hr	slope m/m	inlet width m	dimensions m×m
Large flume	0.25–1	0.2–1	0.0055–0.01	0.25	10×3
Stream table	1	1	0.01	0.1	5×1.25
Delta table	0.17	0.6	0	0.04	1.5×1
Friedkin channel	0.111	0	0.01	0.05	1.1×0.05

10
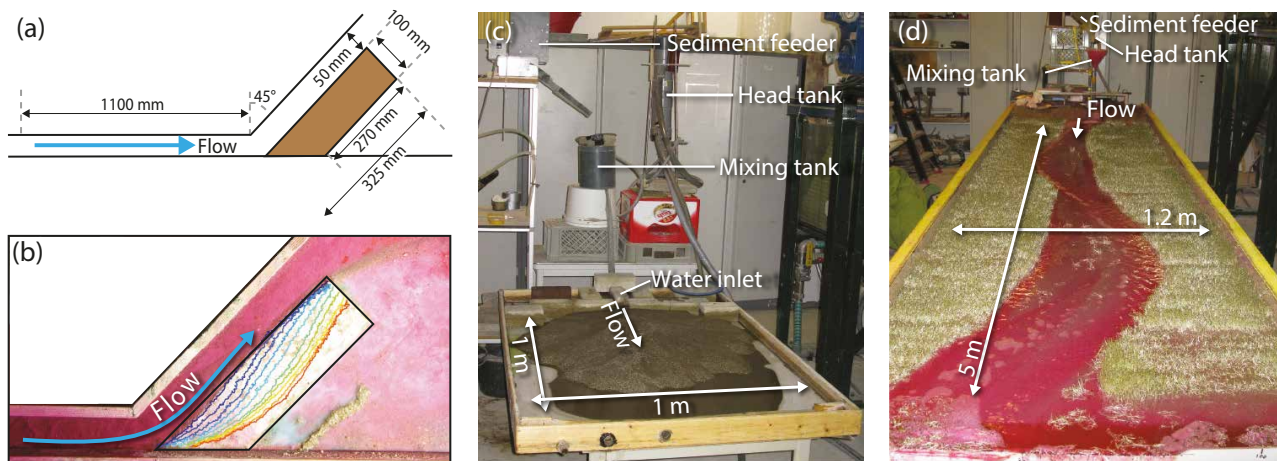
Figure 2: *Small scale experimental setups to systematically test erosional and depositional behaviour for different sediment mixtures under conditions similar to that in large flume experiments (see Table 2). A. Setup of Friedkin erosion test. The water supply channel is 5.0 cm wide, 1.1 m long and coated with a sand layer to represent sand roughness. The standard mold has a surface area of 3.225 dm² (or ×10⁻² m²), is 2 cm in height (total volume 0.645 L) and is inclined with a 45° angle to the water supply channel. B. Friedkin erosion run with erosion indicated for every time step. Warmer colours correspond to a longer erosion duration. C. Side view of Delta experiment. We used a flat plywood stream table of 1.5 by 1 m with a constant base level with a 4.0 cm wide inlet. (d) Side view of plywood stream table of 5 m long, 1.25 m wide set at a slope of 0.01 m/m.*

deposit at all but percolated in all directions. As a result, the entire deposit becomes strongly cohesive when PHPA is used. This need not be a problem in the case of accumulating deltas where deeper layers do not affect the morphodynamics. However, in the case of non-aggrading conditions, such as river patterns experiments on a fluvial plain of constant slope and elevation, it prohibits morphodynamics due to the large cohesion added to sediment.

Figure 3: *Particle size distribution of four sediment mixtures; uniform sand (black-solid line), poorly sorted sand (red-dashed line), 20% silt mixture (blue dash-dotted line) and 40% silt mixture (greed-dotted line). The cutoff size (D_{cp}) shows the fraction that will percolate into the bed. Porosity (ϵ_{tot}) indicates the percentage of pores in the sediment mixture.*

Vegetation was sown on the poorly sorted sand in some experiments to simulate a uniform vegetation distribution, and added to the inflow in other experiments, which is a novel approach that simulates how the flow distributes vegetation on the morphology (Van Dijk et al., 2013a). We experimented with various species (Van de Lageweg et al., 2010), including garden rocket (*Eruca sativa*), garden cress pepper weed (*Lepidium sativum*), thale cress (*Arabidopsis Thaliana*) and alfalfa (*Medicago sativa*) as in Tal and Paola (2009) and Braudrick et al. (2009). Sprouts of these species were systematically subjected to different seeding densities and to various growing conditions, including light intensity, submergence and nutrient starvation. We found that plants sprouted quickest and grew best on saturated soil. Garden cress pepperweed and garden rocket grew the largest stem heights and root systems, whereas thale cress and alfalfa remained smaller and grew slower. Alfalfa and garden rocket developed single main roots, whereas garden cress pepper weed developed main roots with side branches that anchored much more strongly in the soil. Denser seeding reduced sprout growth after about a week. Stronger light increased plant growth and plant strength. A striking result was that environmental conditions do not affect seedlings very much in the first week because in this stage the plants still depend mostly on nutrition from the seed. However, the sand is devoid of nutrients, which leads to general mortality after a week, particularly if water is not refreshed but recirculated.
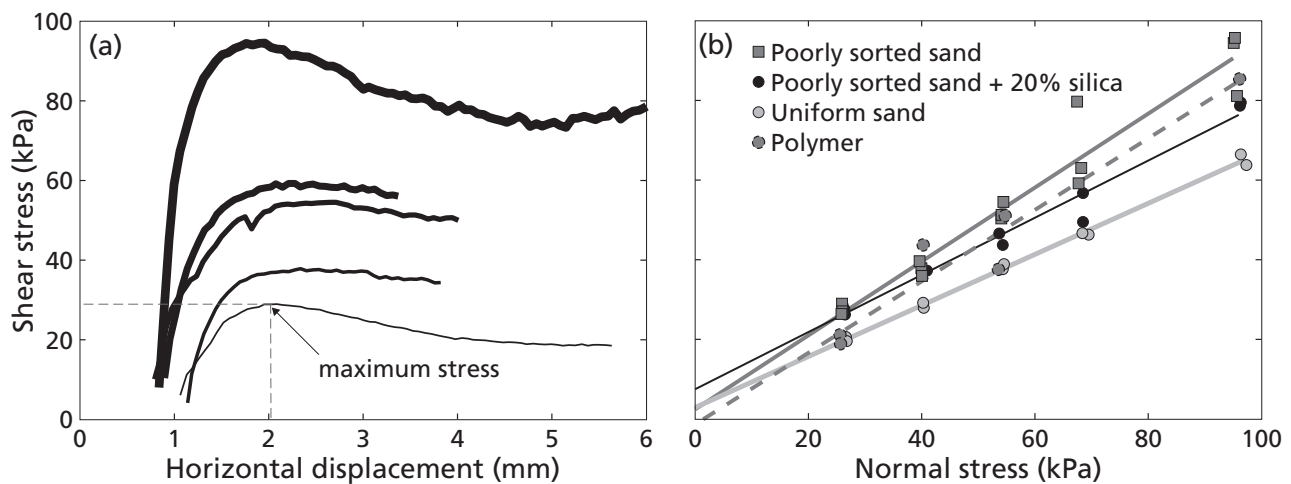
Figure 4: *Results of direct shear tests. A. Typical time series of required shear versus displacement showing the optimum before failure. B. A fit of the maximum strength at failure for replica measurements and different normal stresses, but note that these normal stresses represent bank heights orders of magnitude larger than found in experiments. The sediment mixture with silica flour has significant cohesion whereas the polymer mixture (poorly sorted sediment with 20% silica to which polymer is added) shows a negative apparent cohesion. See Fig. 3 for compositions.*

Fungi developed on dead plants when water was re-circulated in a relatively dark laboratory, but these can be prevented or slowed in development by using fresh water and a minor amount of copper sulfate. We had mixed results with grow lights which may lengthen the life (Braudrick et al., 2009) but may also dry the plants out too much.

3.2. Direct shear test for material strength

Experiments using clay for floodplain material demonstrated that this material is too strong to be removed by experimental rivers (Jin and Schumm, 1987). This outcome is expected because clay has a strength of the order of several kilo-Pascal, whereas the flow shear stress in nature is of the order of several Pa and less in the laboratory. Many past efforts to reproduce river patterns in the laboratory focussed on finding and optimising a floodplain-forming material or using vegetation as a 'floodplain filler' (Gran and Paola, 2001; Tal and Paola, 2007; Braudrick et al., 2009). Plants increase bank strength as do cohesive floodplain sediment and vegetation in nature (Tal and Paola, 2007), but this effect has not been quantified relative to other materials. Predictions with theory or models for bank stability cannot replace measurements because they are strongly dependent on empirical determination of cohesion and other soil parameters, as well as physical properties of plants with roots in that soil.

A classic geotechnical measurement of material strength is the direct shear test in saturated and well-drained conditions, which we used to compare strength of materials used in experiments. Samples 0.06 m wide and long and 0.02 m thick were sheared at a constant rate and under a constant normal stress whilst the required force was measured. The di-

rect shear apparatus incorporated a motor to move a piston at a predefined constant rate (horizontal displacement). A load hanger system provided the adjustable (5, 10, 15, 20 and 30 additional kg) normal stresses. The material strength was derived at the peak shear strength just before failure (Fig. 4a). For every sediment sample at every normal stress at least three replicates were measured. The intercept of the trend line of shear strength against normal stress is an apparent cohesion (c'), and the slope of this trend line indicates the angle of internal friction (ϕ).

We found that accurate measurements of shear strength require a significant normal stress, but then the extrapolation to zero normal stress for the determination of cohesion is inaccurate (Fig. 4b). Although the apparent cohesion of poorly sorted sand with silica flour is larger than that without the silt, the uniform sand also has a relatively large cohesion value. On the other hand, sand with polymer has a negative apparent cohesion, if a straight line is fitted, because the polymer limited drainage from the sample making it unsuitable to quantify its material strength from a direct shear test. We also attempted measurements of samples that were rooted with alfalfa and garden rocked but this gave irreproducible results because roots were pulled through the sediment.

Apparently the material properties at the experimental scale differ significantly from that in the direct shear test. A normal stress of 25 kPa, the minimum value applied here, means that a sample of unit surface area is subjected to a weight of 2500 kg. With a typical soil density of about 1500 kg/m^3 this translates to a minimum bank height of more than 1 m. The banks of experimental channels are, however, of the order of 0.01 m high. We therefore conclude that the standard direct shear test of material strength is

Table 3: *Sediment mixtures were composed of poorly sorted sand ('Ps'), silica flour ('s-f'), bentonite and/or polymer. Polymer was measured in grams of dry granular material per litre of dry sediment whereas the other components were measured as volumes of dry material. Note that our Delta mix contained much less polymer than other mixtures that also incorporated polymer.*

Input	Ps silica-flour	Ps s-f bentonite	Ps s-f polymer	Delta mix	Hoyal mix	Unit
Poorly sorted sand	80	80	80	79.8	76	% vol
Silica flour	20	20	20	20	19	% vol
Bentonite	-	3	-	0.2	5	% vol
Polymer	-	-	1.25	0.07	1.25	g/L

of limited value for the present purposes.

3.3. Friedkin setup for bank erosion tests

The bank erosion rate resulting from all physical and biological processes acting in channel pattern experiments can directly be measured in an experiment. These processes include flow shear, armouring at the bank toe, capillary forces, added strength by roots and polymer excreted from roots, added flow resistance at banks by overhanging vegetation, mass failure of banks, and so on. We present an experimental 'Friedkin' setup gleaned from Friedkin (1945) with which we compared bank erosion rates for a wide range of conditions and materials of experiments from literature (Table 1). The principle of the experiment is that a block of sediment with similar bank height as in the channel pattern experiments is eroded over time by clear water of similar water depth and flow velocity as in the channel pattern experiments (Fig. 2a). We used a mould to position a block of slightly undersaturated sediment in the Friedkin flume with high accuracy and repeatability. The walls of the block of sediment were initially vertical for easy mold removal and stayed vertical because of adhesion of the moist material. Time lapse photography and image analysis allowed for automated determination of the volume of the block of sediment (Fig. 2b). Each time series of sediment volume was characterised by a half-life time at which half the sediment was eroded.

Tens of small-scale bank erosion experiments and bank failure experiments (Van de Lageweg et al., 2010) were performed to quantify the strength of banks reinforced by plant roots at the experimental scale. Seeds were allowed to sprout in sand already positioned in moulds to prevent disturbance upon placement in the flume. Various mixtures of sediment were tested repeatedly with systematically varying cohesive additions (Table 3).

We found different erosion trends that were very sensitive to material composition (Fig. 5). Many erodible mixtures show relaxation behaviour characterised by fast initial erosion and gradually decreasing erosion rate (Fig. 5a). Some materials, such as our standard poorly sorted sand (Fig. 3) continued to be eroded until the block of sediment was breached. Breaching is important to have as a condition con-

trasting cases where the breach did not occur because of different material properties. For example, in very poorly sorted sand with a tail of fine gravel with a 90th percentile of 2.7 mm static armouring occurred at the bank toe, which prevented breaching. The uniform sand of van Dijk et al. (2009) with the hydraulically smooth boundary showed a constant bank erosion rate rather than relaxation, possibly because it is fine and highly mobile in the experimental range of shear stress. The polymer 'delta' mixture with bentonite and poorly sorted sand of a lower concentration than the mixture of Hoyal and Sheets (2009) (Table 3) was moderately erodible, whereas a mixture of poorly sorted sand with silica flour and higher bentonite concentration was hardly erodible (Table 3).

The effect of silica flour was tested for two different sedimentary styles: uniformly mixed into the bed to represent a heterogeneous bank with many thin layers of cohesive sediment, and spread (as dry powder) as a uniform cohesive silt on top of a uniform cohesionless layer of poorly sorted sand (Fig. 5b). The erodibility of the sediment block was more than halved by increasing silt to 40% by volume. This is more than the pore volume of the poorly sorted sand, so the mixture must have become matrix-supported on the silt between 20–30% (Fig. 3). Indeed, we found that dry mixing followed by wetting worked well whereas wet mixing led to immediate fluidisation upon removal of the mould. However, exceeding the pore volume when mixed dry seems not to have affected the erodibility, except perhaps that variability was much larger for 40%.

For the second style with a uniform silt layer on top of cohesionless sand the volumetric fraction of silt was calculated from the thicknesses of sand and silt layers to be able to compare on the same axis to the uniformly mixed banks (Fig. 5b). A layer of silt on a sandy bank doubled the half-life compared to the same amount of silt mixed uniformly into the sand, and increased variability of the half-life. A 1.5–2 mm layer of silt resulted in a half-life of 2–3 hr which is considerably longer than for the control experiments with poorly sorted sand which breached in less than 0.5 hr. This shows that an experimental floodplain with a top layer of silt considerably reduces bank erosion rates even though the bank toe is composed of cohesionless sediment. We suspect that
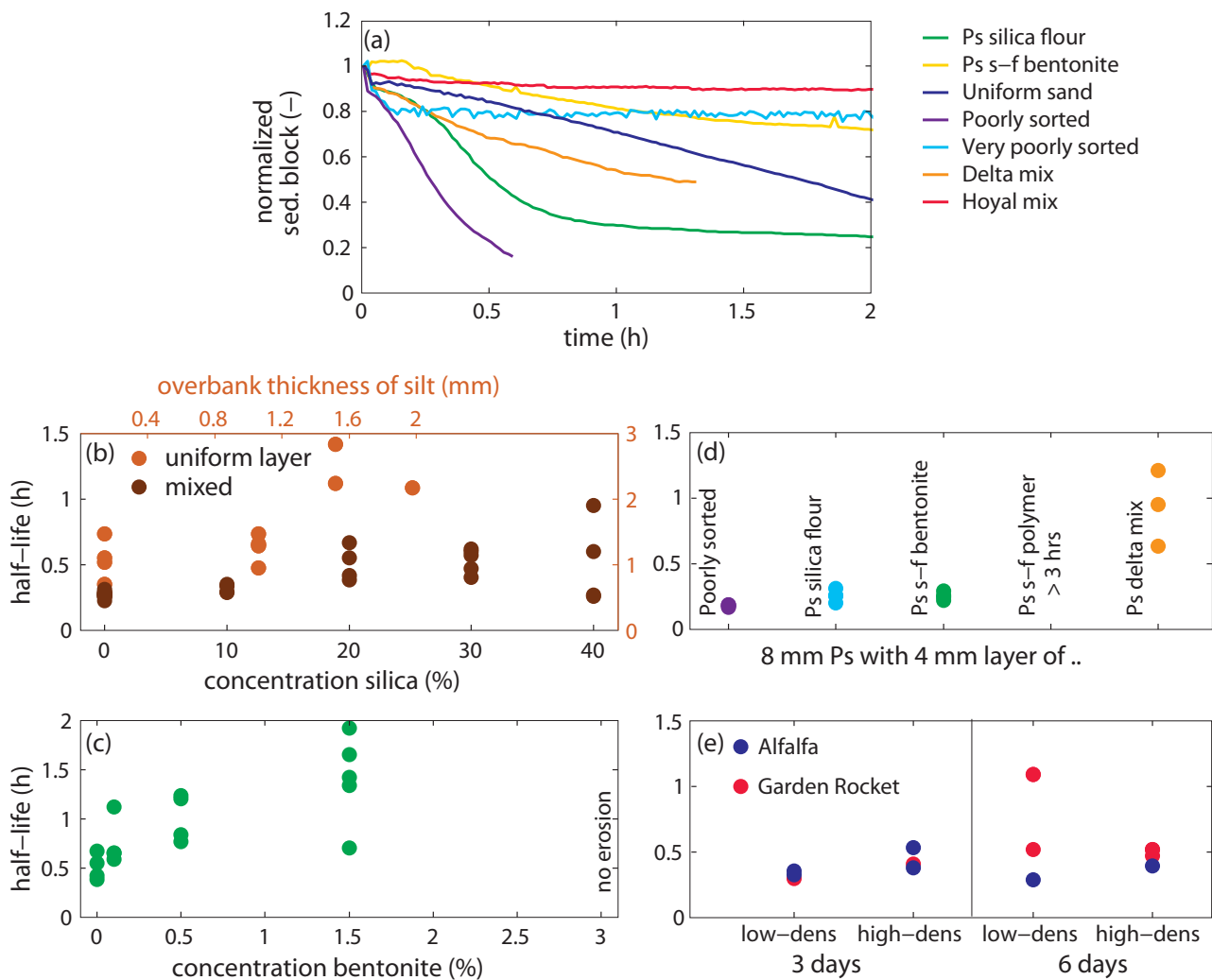
Figure 5: *Bank erosion tests results (see text). 'Ps': poorly sorted sand, 's-f': weakly cohesive silt-sized silica flour. A. Time series of normalized sediment volume shows different behaviour of materials (Fig. 3, Table 3). B. Half-life (in hours) of sediment blocks with silt mixed uniformly into poorly sorted sand (given as a volumetric concentration) or deposited as a uniform layer on top of poorly sorted sand, plotted such that the total amounts of silt in the cases of a uniform layer on top of sand and silt mixed into the sand are the same. C. Half-life time of the sediment block with 20% silt and increasing bentonite concentration. D. Half-life of an 8 mm base layer of poorly sorted sand with a 4 mm top layer of different compositions. E. Effect of two plant species, two plant ages and two seeding densities on bank erosion.*

the relatively large effect of the top layer is partly caused by a transition from hydraulically rough to smooth boundary of the bank toe as silt blocks fail from the bank top and gradually break apart on the bank toe to enrich the sediment surface locally with silt. The silt blocks themselves seemed not to prevent bank toe erosion.

As expected, bentonite had a much stronger effect on bank erodibility than silica flour (Fig. 5c). A concentration of only 1.5% by volume halved the erodibility and at 3% no erosion occurred at all. The bentonite is an important component of the polymer mixture of Hoyal and Sheets (2009) because it reacts with the polymer, but the Friedkin experiment shows that the bentonite on its own must have a large effect compared to the much less cohesive and coarser-grained silica flour used in the fluvial experiments of Peakall et al. (2007) and Van Dijk et al. (2012). The

effect of polymer mixed into the sediment in the concentration used by Hoyal and Sheets (2009) is much larger than any other component tested here. We also tested the effect of 4 mm thick layers of cohesive sediment on a 8 mm thick bank compared to the control experiment with 12 mm thick poorly sorted sand (Fig. 5d). Poorly sorted sand with 20% silt by volume is two times less erodible than cohesionless poorly sorted sand. Further addition of the same amount of bentonite as in the delta mixture of Hoyal and Sheets (2009) adds no measurable effect. However, addition of the same polymer concentration as in Hoyal and Sheets (2009) renders the banks nonerodible as tested over more than 3 hours. Our delta mixture, which combines silica flour, bentonite and a much lower polymer concentration was somewhat erodible but had a half-life much longer than the poorly sorted sand and the silica flour mixture.

Again we found that the polymer percolated from the top layer into the entire bank which increased the strength of the initially cohesionless material as well. This behaviour shows that the polymer is unsuitable for river experiments since the risk of ossification is large and we found no way to fix most polymer to sediment and stop percolation. We observed that mixtures and deposits aged within hours and became much more cohesive in the ageing process, but we did not investigate in detail the development of gelling by the polymer. There exist oxidants that break down highly-gelled muds with polymer which may be interesting to evaluate in future investigations.

Erodibility of vegetated banks is strongly determined by seeding density, rooting density and depth of rooting relative to channel depth (Fig. 5e). Halving the seeding density approximately doubles the erodibility for 3-day old seedlings, with no difference between the two species shown. However, after 6 days the garden rocket provided much more strength to the bank than alfalfa, but only for the low seeding density, because the roots branched strongly in these conditions. For the higher seeding density the effect of the two species hardly differed and also was the same as after 3 days. The enhanced bank strength for low garden rocket seeding density is probably due to the strongly spreading root systems of individual seedlings in contrast to that of alfalfa. Apparently high alfalfa seeding densities can compensate for the strength added by root branching of garden rocket, producing differences between species for low seeding densities. However, Braudrick et al. (2009) found that after two weeks also the root density of alfalfa increases. Nevertheless these results suggest that bank strength by alfalfa is the less difficult to control because it merely depends on seeding density. In addition, the erosion tests of the vegetated banks indicate that the risk of ossification is large and therefore low seeding densities and limited spreading root systems of individual seedlings are preferred.

We conclude that the Friedkin setup is useful to compare bank erosion rates between various sediment mixtures and to isolate effects of additions such as cohesive material or plants, and to test layered bank scenarios.

3.4. Delta setup for sedimentation tests

Erosion and sedimentation are equally important: to maintain a constant width in time, the bank erosion must be equalled by sedimentation on the opposite side of the river. 'Sedimentation' is also the set of processes that determines the stratification once fluvial accommodation space has been generated by a channel or by subsidence. Here we present an experimental 'Delta' setup that allows fast and systematic comparison of sedimentation styles of different materials. Stratification will obviously differ between deltas and floodplain splays, but the sedimentary behaviour is similar in the sense that there is an expanding flow that leads to sedimentation, and there is also channel initiation and bifurcation as in splays, chutes and braided rivers.

Formation of small-scale channelised fan deltas in the laboratory has proven challenging but significant progress has been made in several labs in recent years (e.g. Sheets et al., 2002; Hoyal and Sheets, 2009; van Dijk et al., 2009; Powell et al., 2012). Various types of deltas have been created, ranging from fine- to coarse-grained, non-cohesive to cohesive, and from sheet flow dominated to strongly channelised. These experiments have elucidated a number of important factors and autogenic behaviours under constant boundary conditions, such as channelisation and mouth bar formation and backward sedimentation leading to avulsion. However, there has been very little systematic investigation of scale effects and of the effect of sediment mixture on autogenic delta behaviour. Here we describe a set of experiments with identical conditions to investigate the link between sediment mixture properties, such as grain size, sorting, addition of fines or polymers, and delta morphodynamics. A quantification of aspects of morphodynamics such as time series of channel dimensions, network pattern, planform delta shape, and bifurcation mechanisms is beyond the scope of this paper. Visual inspection, however, strongly suggested that the sedimentary behaviour and the tendency to form channels can also be expected in large-scale experiments. These experiments were designed to be small, fast and repeatable, so that a wide range of different mixtures could be covered.

We found that the delta experiments elucidated the tendency of splay formation and channelisation in naturally formed sediment deposits. Sedimentation patterns and dynamics differed dramatically between different types of sediment (Fig. 6). The uniform fine sand invariably exhibited sheet flow or formed unwanted scour holes because of hydraulic smooth conditions. These scour holes are unwanted because their dimensions are nearly independent of channel depth and often much larger than channel depth. We further found that deltas with the uniform sand exhibited alternating phases of (unchannelised) sheet flow and deeply incised channels (Fig. 6a) in agreement with van Dijk et al. (2009); Van Dijk et al. (2012). Incision initiated with a scour hole at the apex.

In contrast, the poorly sorted sand formed well-channelised deltas without scour holes, probably because the coarser particles cause hydraulically rough conditions (see Eq. 8), and because bifurcations were temporarily stabilised by gravel deposition (Fig. 6b). More mature deltas were generally semi-circular fan-shaped with protruding mouth bars.
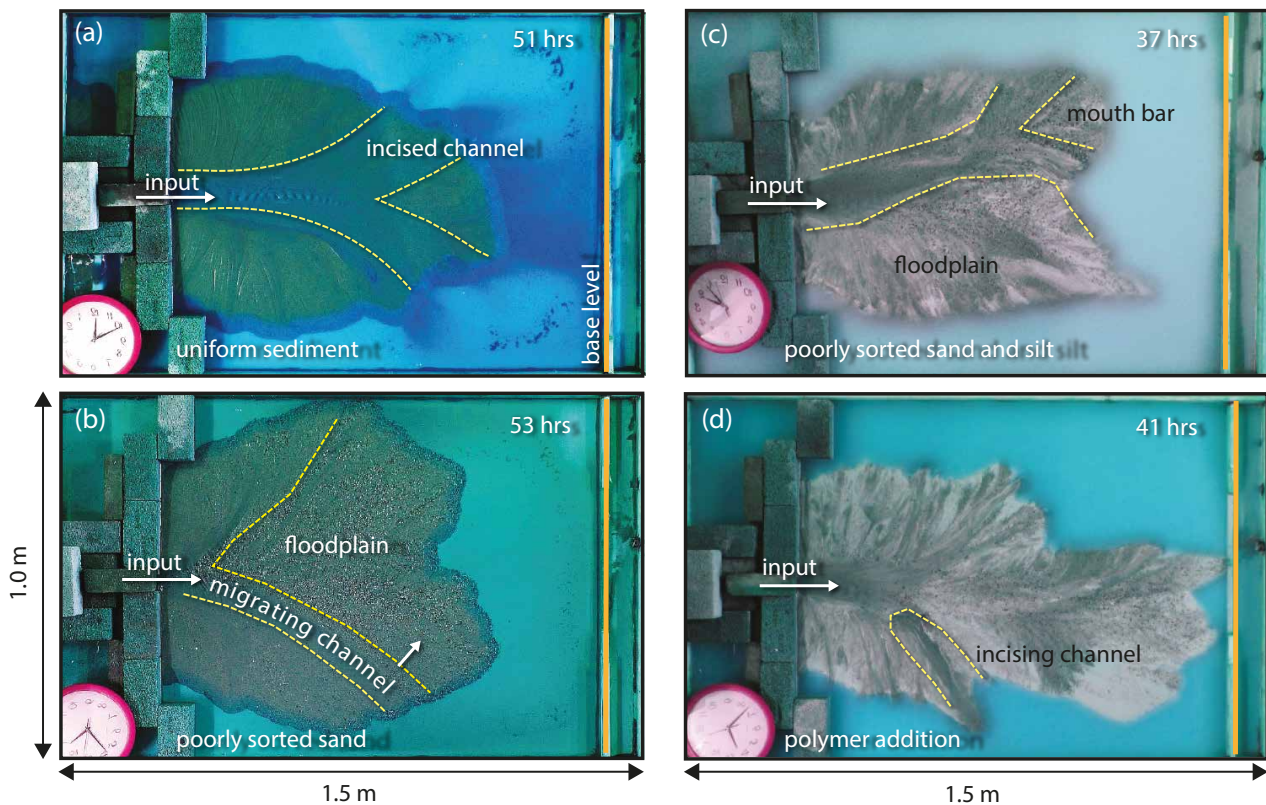
Figure 6: *Delta morphology. A. Uniform sand experiments show delta development with cycles of sheet flow and channel incision (as in van Dijk et al., 2009). B. Poorly sorted sand experiments show sediment size-sorting trends, mouth bars and multiple channels which migrate until they are abandoned. C. Silt addition results in a more focussed channel, at the end of which a mouth bar forms that leads to back-sedimentation and channel back-filling followed by avulsion (as in Hoyal and Sheets, 2009; van Dijk et al., 2009). D. Polymer addition to the sediment mixture (poorly sorted sand with 20% silt) results in back-cutting of relatively narrow and deep channels and much more irregular deltas (see also Hoyal and Sheets, 2009).*

Weakly cohesive silica flour added to the poorly sorted sand increased channelisation and channel depth (Fig. 6c). The channels showed lateral migration as well as 'avulsive' tendencies in the form of chute cutoffs, and deposited silt-rich sheets between channels in agreement with the river experiments with similar sediment by Peakall et al. (2007) and Van Dijk et al. (2012). A wide sediment mixture with polymer, poorly sorted sand, silica flour and in some cases bentonite (Table 3, delta mix) formed narrow channels with limited lateral mobility and strong banks (Fig. 6d). Channels were narrower than in any other mixture and flow was often supercritical. As a result of channel extension by mouth bars and upstream aggradation, avulsion occurred frequently in agreement with Hoyal and Sheets (2009). At the largest polymer concentrations, knickpoints and backward steps appeared similar to those in deltas on cohesive lake beds or bedrock. The polymer percolated to underlying layers which became stronger over time. Experiments with higher concentrations of polymer and bentonite (Table 3, Hoyal mix) failed in our setup because the delta apex built up to a level exceeding our simple wooden inlet. Furthermore the properties and ageing of this material are determined partly by the setup that mixes polymer into the flow and sediment feed affects.

In general, these experiments showed that poorly sorted sediment removes the unwanted scale effect of scour holes in fine sand and facilitates sorting-related bifurcation and bar formation. Addition of silica flour increases channelisation by strengthening the banks. Addition of polymer increases bank strength much more and enhances channelisation and avulsion, but causes unwanted channel bed hardening and backward step erosion. In aggradational settings this condition may not be a problem but in river pattern experiments without net degradation or aggradation the polymer would inevitably ossify the entire system.

3.5. Stream table setup for bar formation

A stream table was used to study morphodynamics resulting from the combination of erosive and sedimentary processes without net degradation or aggradation. In our channel pattern experiments, the stream table accommodated about two bar or meander lengths. Water and sediment were supplied at the upstream boundary and the downstream boundary was a fixed weir. Overhead photography captured the morphodynamics, and dye indicated water

depth and active channel flow. The stream table allowed fast experimentation with one or two experiments per day and rapid preparation within an hour for new experiments because of its small size. Different sediments were tested and variations in upstream discharge and sediment feed were applied to test theoretical relations between bar wavelength and discharge and to determine the equilibrium conditions. Furthermore, vegetation was manually sown on the initial bed or in other experiments added to the inflow and allowed to be spread by flow. In this setup we discovered that shifting of the inlet funnel was crucial to maintain channel dynamics, which was later employed in the large flume experiments (Van Dijk et al., 2012; van de Lageweg et al., 2013a).
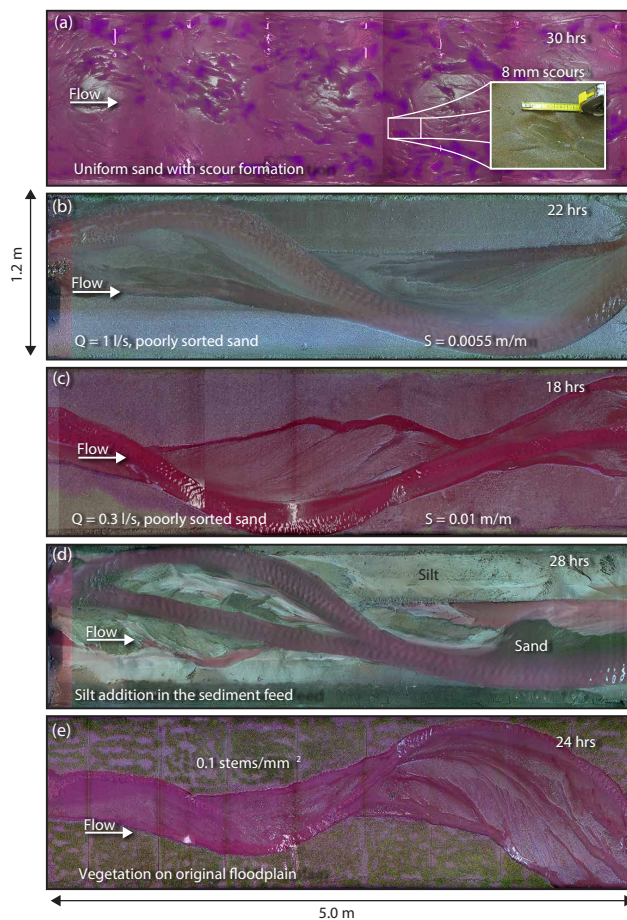
Figure 7: *River morphology. A. Uniform sand leads to hydraulically smooth conditions which show scours and ripple dunes in the bed. B. In the poorly sorted sand initial meander bends develop until the sides are reached. C. A decrease in discharge led to an incipient meandering river, which shows a cutoff before the bends had grown to the sides of the flume. The lower discharge did not decrease the dynamics of the experiment. D. Silt addition in the feed deposited on the outer bank floodplain and in the inner bank point bar. E. Vegetation on the initial floodplain shows formation of sharper and shorter bends, when the bank stability increases.*

As in the delta experiments we found that uniform sand had many scour holes but did not develop an obvious channel (Fig. 7a), which is expected from hydraulically smooth conditions. A double, weakly sinuous bend developed in poorly sorted sand with an upstream perturbation (inflow at an angle to the general flume direction). This system also formed scroll bars visible from the sediment sorting pattern (Fig. 7b). A large reduction of discharge resulted in smaller channels, which then exhibited chute cutoffs before the bends migrated into the sidewalls, which was a reason to stop the experiments with higher discharge (Fig. 7c). Addition of silt to the feeder led to incipient floodplain formation, somewhat narrower channels, and in some cases to inhibition of chute cutoff (Fig. 7d). High silt concentrations in the feed and lower concentrations in the initial bed both led to decreased lateral mobility or even immobility. Finally, we show an example of an experiment with alfalfa vegetation sown uniformly on the initial floodplain, which reduced lateral mobility but also caused sharper and shorter bends and higher scroll bars (Fig. 7e).
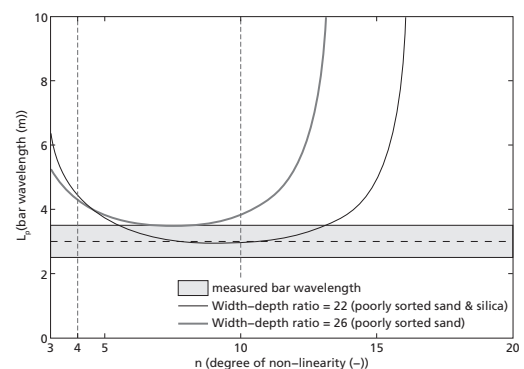
Figure 8: *Comparison of measured bar wavelength in stream table experiments (Fig. 7) and predicted bar length (Eq. 12), which is sensitive to transport nonlinearity and which is highly variable near the initiation of sediment motion. The choice of $n = 10$ recommended by Crosato and Mosselman (2009) for gravel-bed rivers agrees reasonably well with our results.*

The wavelength of the forced bends in one of the stream table experiments (Fig. 7b) was directly compared to the value predicted by theory (Eq. 12, Fig. 8). The wavelength is well predicted, but the prediction is highly sensitive to the assumed nonlinearity n of sediment transport, which is highly variable close to the initiation of sediment motion as in these experiments. On the one hand this shows that there are no apparent scale effects in the overall dimensions of the bends in the sense that the vertical distortion renders the theory inoperable as suggested by Struiksma (1986). On the other hand it shows that the predicted wavelength has considerable uncertainty. Hence the stream table experiments allow an accurate empirical determination of the wavelength for the used conditions and sediment that can aid designing a large-

scale experiment. Ultimately, these small-scale experiments resulted in the set of boundary conditions and sediment mixture used in our large flume experiments (Van Dijk et al., 2012, 2013b; van de Lageweg et al., 2013a).

4. DISCUSSION

4.1. Experimental design to represent natural rivers

We presented a combination of theoretical and empirical designs for river and delta experiments. The theoretical design is based on classical similarity scaling and the empirical design on a set of experiments that can be conducted quickly and cheaply to explore sediment behaviour on bank erosion in the Friedkin setup and on channelisation and floodplain formation in the Delta setup and the stream table so that the large-scale experiments can be conducted more efficiently.

We compared behaviour of materials used in the literature, including poorly sorted sediment, silt, clay, alfalfa and a polymer. It turns out that aggrading delta environments are less sensitive to materials with a large threshold for erosion, particularly the polymer. However, river environments in dynamic equilibrium require a more subtle mode of floodplain building, which can be done by silt, light-weight sediment, alfalfa and combinations thereof. On the other hand, materials used here for the fluvial experiments could also fruitfully be used for delta experiments in the future and would perhaps lead to enhanced floodplain formation in deltas. Furthermore, there are opportunities for cross-fertilisation with other fields that employ experiments with mobile sediments, including coastal wave-driven sediment transport (Hassan and Ribberink, 2005), debris flows (e.g. Goujon et al., 2007; D'Agostino et al., 2010; Iverson et al., 2010), turbidites (e.g. Postma et al., 2009; Eggenhuisen and McCaffrey, 2012), tidal experiments (e.g. Tambroni et al., 2005; Stefanon et al., 2010; Kleinhans et al., 2012) and planetary experiments with sediment flows, surface runoff and groundwater outflow (e.g. Kraal et al., 2008; de Villiers et al., 2013; Marra et al., 2014).

The most important characteristics of natural rivers are that the sediment has to be mobile, the channel bed sediment must be cohesionless and on average coarse enough for hydraulically rough conditions, and flow must be subcritical. Furthermore the erodibility of the banks and the resulting width-to-depth ratio determines natural bar pattern (Fig. 9). These characteristics are also the most important experimental design criteria. Most experiments listed in Table 1 fulfill these criteria, except those with the finest bed material. A striking result is that most experiments have dominantly bedload transport for sandy sediment, whereas natural rivers with sand as bed material are usually dominated by suspended bed-material transport. Thus, most experiments to date represent gravel-bed rivers in nature, whereas experimental reproduction of suspension-dominated sand-bed rivers remains a challenge. Perhaps the use of light-weight sediments coarse enough to prevent hydraulically smooth conditions and cohesion can be of use.

4.2. Interpretation of experimental scales

Given a spatial scale of an experiment designed according to the rules of the similarity scaling procedure, a morphological time scale can be calculated directly from a relevant sediment transport rate and a control volume that is eroded or deposited. For our experiments and analogue models that violate similarity scaling rules this time scale approach is still valid because the sediment transport rate literally determines how fast a certain volume is filled or removed. However, the process of bank erosion depends on multiple variables including geo-technical properties. This raises the question how the characteristic time scale of channel migration and bend formation a river pattern experiment should be determined, and what it actually represents.

We compared experimental bend migration rates normalised with channel width to typical values found in nature. Typical bank erosion rates in the experiments were of the order of 1 cm/hr, or about one channel width per 8 floods (Van Dijk et al., 2013b). Apparently, the experimental channel migration is relatively faster than in nature. In itself this is not entirely surprising because experimental rivers are always in the formative flood condition, so a correction of the data with an appropriate flood intermittency could perhaps correct the bias. To estimate the morphological time scale, a control volume of eroded sediment was calculated from the average water depth near the outer banks and the surface area of the area eroded by one bend with the maximum erosion length of one width. This volume, eroded over a certain amount of time, was compared to the sediment transport feed rate of the experiment. We found that migrating bends reworked a surprisingly large amount of sediment: more than four times the sediment feed rate (Van Dijk et al., 2012). This agrees with values found in the Friedkin experiments, where no sediment was fed upstream.

At the moment the cause of the relatively large local sediment transport rate in eroding bends is not fully understood. Higher transport rates near the banks are expected to some extent because flow shear stress is larger than average near the outer banks and transport is enhanced by the bank slope. On the other hand, the banks are stronger than the loose bed sediment. Perhaps the high transport rate is due to
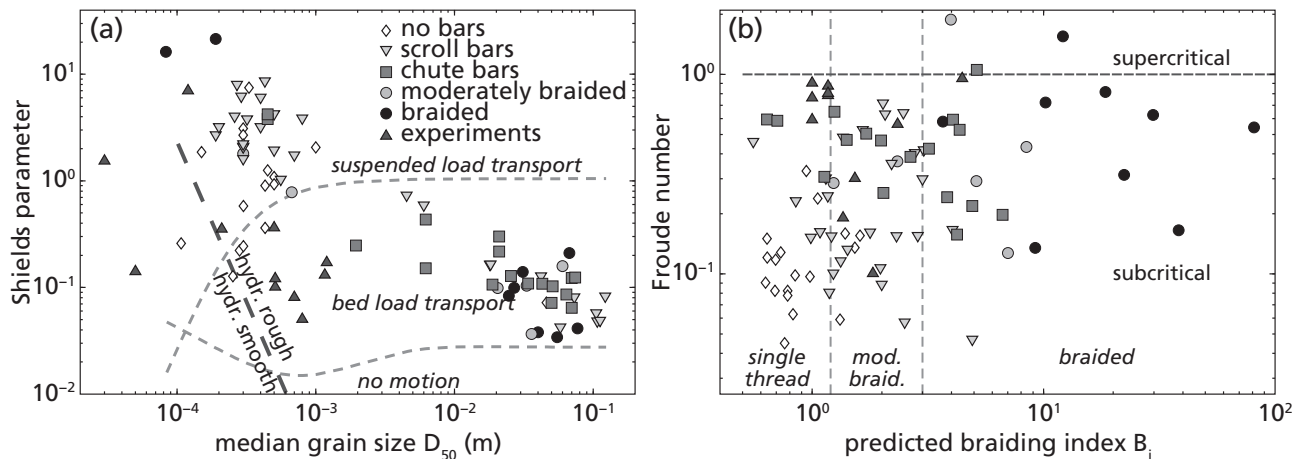
Figure 9: *Comparison of parameters most relevant for river patterns in experiments (Table 1) and natural rivers (Kleinhans and van den Berg, 2011). A. Dimensionless shear stress as a function of particle size. The thresholds for motion and suspension, and the transition from hydraulically smooth to rough at Re* = 5 (Eq. 8) are indicated. B. Froude number as a function of braiding index, predicted with Eq. 19 (see Kleinhans and van den Berg, 2011, for definitions and data).*

an experimental scaling issue where banks in experiments are weaker than in natural rivers relative to the shear stress of the outer bank flow, but perhaps the sediment displacement rate by bend migration in nature is also much larger than the typical average sediment transport rates in the channel.

Tentatively, we define an approximate time scale characteristic of bend migration over which a bend migrates on average one channel width. Here we compare the experiment of Van Dijk et al. (2012) to the Allier river in France and the Rhine River near the Dutch-German border, which are both morphologically similar to the experiment in the sense that the dominant mode of sediment transport is bedload and the pattern is meandering with chute cutoffs. When compared to the Allier River, the experiment represents decades and when compared to the Rhine river it represents centuries. Rivers of other sizes would have different time scales depending on their dimensions, sinuosity and on general floodplain properties that determine bank strength.

4.3. Scale-dependence or independence?

The use of experiments to study fluvial and deltaic patterns has been eloquently defended elsewhere (Paola et al., 2009) and our results in small-scale flumes show that scaling rules from engineering may be violated with usable results for the purpose of studying the patterns if direct comparison to a particular prototype is not the aim.

Paola et al. (2009) argued that experiments of fluvial and deltaic patterns show similar morphology and dynamics as their counterparts in nature, because these patterns are scale-independent. We further assume in agreement with Paola et al. (2009) and others that appropriate experimental morphodynamics automatically lead to appropriate stratigraphy. This assumption is based on the scale-independence of the transverse bed slope predictor (Eq. 20, Van Dijk et al. (2012)) which determines the angle of lateral accretion surfaces and the scour depth of pools. Following Paola and Borgman (1991) the deepest scours determine the set thickness statistics, and our experiments corroborated this hypothesis for meandering rivers (van de Lageweg et al., 2013a). We found that transverse bed slopes in the experiments agree very well with theory (Eq. 20, Van Dijk et al. (2012)) and have values similar to the targeted prototype rivers (Fig. 10). Such results indicate that scale problems of river and delta models may be less problematic than anticipated in the engineering literature.

There is further evidence for scale-independence in field data of natural equilibrium rivers with various patterns (Kleinhans and van den Berg, 2011). Three bar patterns associated with increasingly larger width-to-depth ratios are compared in Fig. 11. The data shows that similar patterns occur in rivers with discharge varying more than three orders of magnitude. For example, rivers with scroll bars and chute cutoffs and formed experimentally in Van Dijk et al. (2012) scale with those for mean annual flood discharges ranging from 20–30,000 m³/s. The ratio of discharge of the largest and smallest rivers in the dataset is as large as the ratio of discharge of the smallest river and the experiments with the same pattern. In other words, similar river patterns are observed for flow discharges differing seven orders of magnitude.
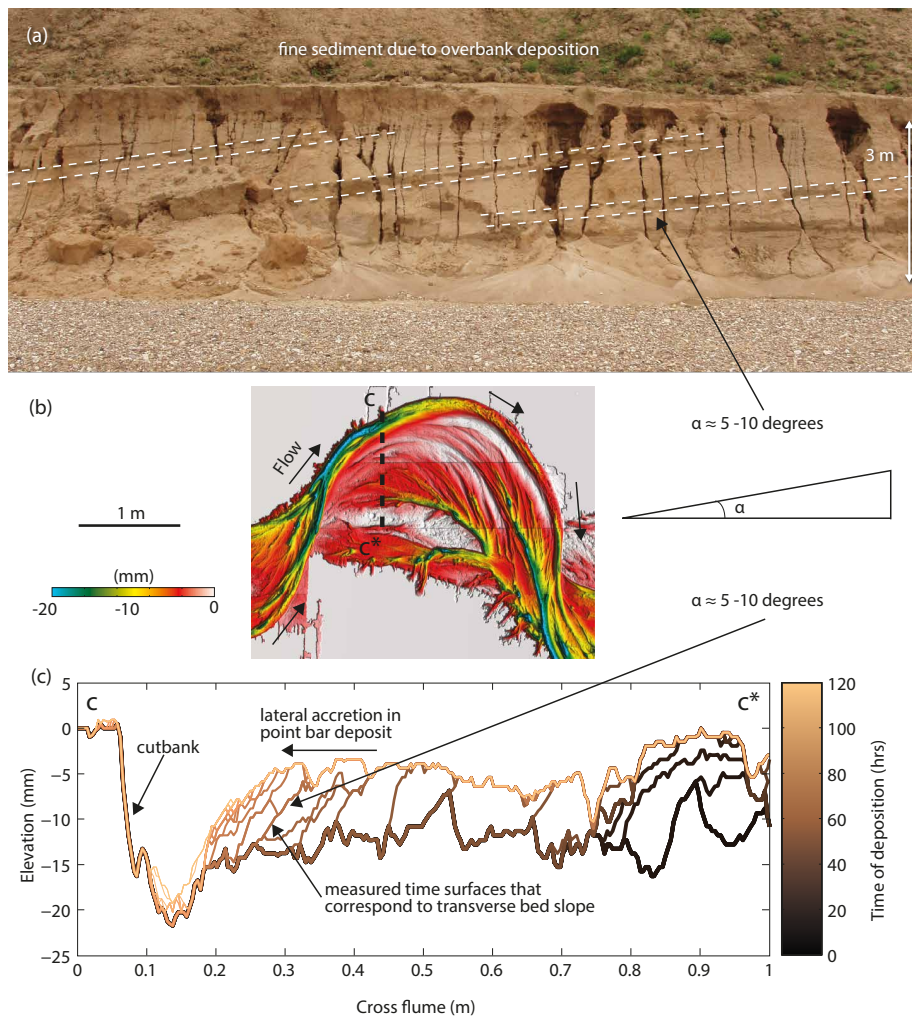
Figure 10: *Point bar deposits have lateral accretion surfaces corresponding to the migrating transverse bed slope of the river channel. A. Section of a point bar deposit of the river Rhine in a quarry in Rheinberg, Germany (courtesy G. Erkens). B. Map view of experimental point bar (Van Dijk et al., 2013b). C. Slice of experimental synthetic stratigraphy of the point bar in B. Lateral accretion surfaces with measured transverse bed slopes agree with theory (Eq. 20).*

The notion of scale-independence is supported to some extent by comparison between experimental data and theoretical predictions of bar lengths and pattern. For example, bar length is well predicted for the small-scale stream table experiments (Fig. 8). However, it is sensitive to the assumed degree of sediment transport nonlinearity, which is highly sensitive to Shields mobility number for initiation of sediment motion. Furthermore the width-to-depth ratio of a laboratory river needs to be about 1.5 times larger than in a natural river in order to develop the same bar pattern. Clearly bars and channels cannot be scaled down without a limit and the patterns are not entirely scale-independent. In fact, most experiments reported in literature (Table 1) have a discharge, particle size and slope of similar magnitude. This is not merely a compromise between the scale effects and the maximum size of facilities that can be handled by a few researchers, but is in fact near the smallest scale above the threshold of motion for medium sand that produces bars, channels and other phenomena of interest.

Clearly, several thresholds exist beyond which the scale-independence breaks down. The theoretical analysis and the experiments show that these thresholds include the transition from subcritical to supercritical flow, the transition from hydraulic smooth to rough bed, the initiation of sediment motion, and the threshold for erosion of cohesive or vegetated banks. Phenomena of interest in their own right arise when these thresholds are not met, but when experiments are designed on the right side of these thresholds, many phenomena found in natural rivers and deltas can be well represented in the experiments in a quantifiable way. Our results show that experiments at practically feasible scales can adhere to these relaxed scaling rules and, in accordance with theory, seem to behave as natural rivers. This implies that laboratory rivers adhering to the relaxed scaling rules can fruitfully be used to explore fluvial morphodynamics and stratigraphy and test theories.
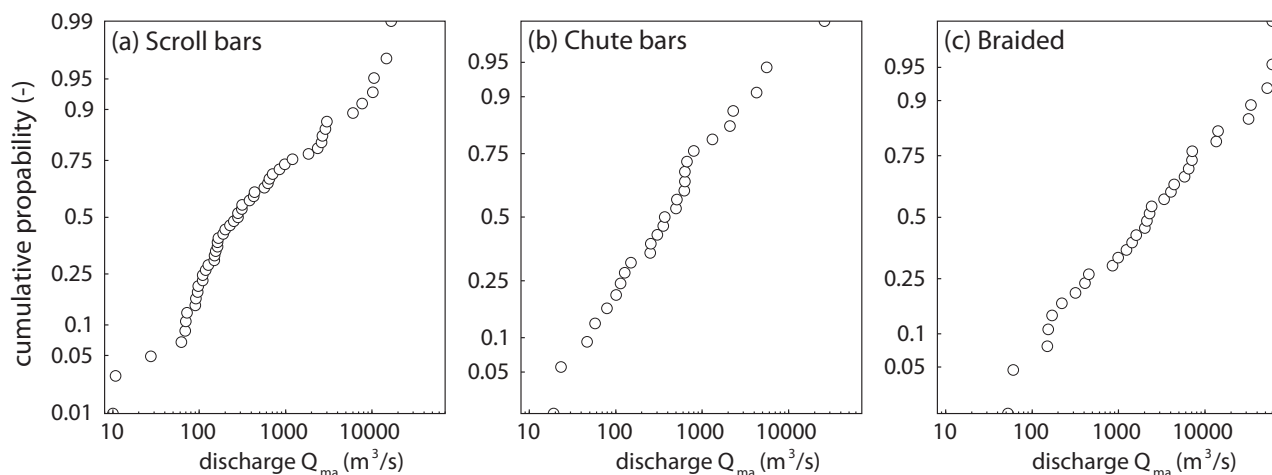
Figure 11: *Cumulative distributions of mean annual flood discharge as a measure for the size of a river, showing that similar patterns occur in rivers with discharge varying more than three orders of magnitude. Field data of natural equilibrium rivers is filtered for bar pattern in three classes that all show evidence of lateral migration: A. Meandering rivers with scroll bars. B. Meandering rivers with scroll and chute bars, and C. braided rivers (see Kleinhans and van den Berg, 2011, for definitions and data).*

5. CONCLUSIONS

We showed how a number of small laboratory setups and protocols can be used efficiently to isolate certain processes, determine their rates and tendency to channelise or spread, assess potential scale effects and identify the most likely successful settings for expensive large-scale experiments. A wide range of materials used in experiments reported in literature were systematically compared.

Similarity scaling has worked well for rivers with fixed banks and for braided gravel-bed rivers, but cannot straightforwardly be applied when width is a dependent parameter in self-formed channels. Physics-based predictors of bar wavelength and transverse bed slope are well applicable without apparent scale problems. However, predicted bar wavelength is sensitive to the assumed exponent in the sediment transport dependence on flow velocity. Bar wavelength can be measured accurately for the experimental conditions on a stream table. We found no indications that the dimensions of experimental rivers and deltas were much distorted compared to real world cases. Rather, the experimental systems have similar morphodynamics and stratigraphy as natural gravel systems, as long as three 'relaxed' scaling rules are adhered to: the sediment has to be mobile, the flow has to be subcritical and turbulent. Most experiments represent gravel-bed rivers in nature, whereas experimental reproduction of suspension-dominated sand-bed rivers remains a challenge.

The tendency of a small-scale fluvial system to form floodplains and erode banks depends to a large extent on the properties of the sediment and presence of vegetation or other substances that enhance bank strength. Traditional mechanical tests of material strength do not yield reasonable results for experimental contexts. Vegetation roots strengthened the banks depending on the seeding density and the age of the vegetation. A slightly cohesive silt, silica flour, added controllable strength to banks of cohesionless sand depending on the volume concentration with which it was mixed into the sand, or depending on the layer thickness at which it was deposited on top of the cohesionless sand. These trends were well quantifiable in the efficient Friedkin bank erosion test, which showed significantly different erosion trends that were very sensitive to the material composition of channel banks. The delta deposition test indicated that sedimentation patterns and dynamics differed dramatically between different types of sediment with an increased channelisation tendency for more cohesive sediment mixtures. Stream table fluvial experiments demonstrate that there is a narrow range of conditions between no mobility of bed or banks, and too much mobility.

The reviewed theory and results show that the rivers and deltas created in the laboratory in landscape experiments seem to behave as natural rivers when the experimental conditions adhere to the relaxed scaling rules identified in this paper, and that required types of fluvio-deltaic morphodynamics can be provoked by conditions and sediments selected on the basis of a series of small-scale experiments.

References

Ashmore, P., 1991. Morphology and bed load pulses in braided, gravel-bed streams. Geografiska Annaler. Series A, Physical Geography 73, 37–52.

Ashworth, P., Best, J., Jones, M., 2004. Relationship between sediment supply and avulsion frequency in braided rivers. Geology 32, 21–24. doi:10.1130/G19919.1.

Bertoldi, W., Zanoni, L., Tubino, M., 2009. Planform dynamics of braided streams. Earth Surf. Process. Landforms 34, 547–557. doi:10.1002/esp.1755.

Braudrick, C., Dietrich, W., Leverich, G., Sklar, L., 2009. Experimental evidence for the conditions necessary to sustain meandering in coarse-bedded rivers. PNAS 106, 936–941.

Carling, P., 1990. Particle over-passing on depth-limited gravel bars. Sedimentology 37, 345–355.

Crosato, A., Mosselman, E., 2009. Simple physics-based predictor for the number of river bars and the transition between meandering and braiding. Water Resources Research 45, W03424. doi:10.1029/2008WR007242.

D'Agostino, V., Cesca, M., Marchi, L., 2010. Field and laboratory investigations of runout distances of debris flows in the dolomites (eastern italian alps). Geomorphology 115, 294 – 304. doi:http://dx.doi.org/10.1016/j.geomorph.2009.06.032.

de Gennes, P., Borchard-Wyart, F., Quéré, D., 2004. Capillarity and wetting phenomena. Drops, bubbles, Pearls, Waves. Springer.

de Villiers, G., Kleinhans, M.G., Postma, G., 2013. Experimental delta formation in crater lakes and implications for interpretation of martian deltas. Journal of Geophysical Research 118, 651–670. doi:10.1002/jgre.20069.

de Vries, M., Klaassen, G., Struiksma, N., 1990. On the use of movable bed models for river problems: a state-of-the-art. International J. of Sediment Research 5, 35–47.

Devauchelle, O., Josserand, C., Lagrée, P., Zaleski, S., 2007. Morphodynamic modeling of erodible laminar channels. Phys. Rev. E 76, 056318.

Eaton, B., Giles, T., 2009. Assessing the effect of vegetation-related bank strength on channel morphology and stability in gravel-bed streams using numerical models. Earth Surf. Process. Landforms 34, 712–724. doi:10.1002/esp.1768.

Eggenhuisen, J.T., McCaffrey, W., 2012. Dynamic deviation of fluid pressure from hydrostatic pressure in turbidity currents. Geology 40, 295–298. doi:10.1130/G32627.1.

Egozi, R., Ashmore, P., 2008. Defining and measuring braiding intensity. Earth Surf. Process. Landforms 33, 2121–2138. doi:10.1002/esp.1658.

Ferguson, R., 1987. Hydraulic and sedimentary controls of channel pattern, in: Richards, K. (Ed.), River channels: environment and process, Blackwell, Oxford, UK. pp. 129–158.

Ferguson, R., 2007. Flow resistance equations for gravel- and boulder-bed streams. Water Resources Research 43, W05427. doi:10.1029/2006WR005422.

Friedkin, J., 1945. A laboratory study of the meandering of alluvial rivers. U.S. Army Corps of Engineers,, U.S. Waterways Experiment Station, Vicksburg, Mississippi, USA.

Frings, R., Kleinhans, M.G., Vollmer, S., 2008. Discriminating between pore-filling load and bed-structure load: a new porosity-based method, exemplified for the river Rhine. Sedimentology , 1–23doi:10.1111/j.1365-3091.2008.00958.x.

Giménez, R., Planchon, O., Silvera, N., Govers, G., 2004. Longitudinal velocity patterns and bed morphology interaction in a rill. Earth Surf. Process. Landforms 29, 105–114. doi:10.1002/esp.1021.

Goujon, C., Dalloz-Dubrujeaud, B., Thomas, N., 2007. Bidisperse granular avalanches on inclined planes: a rich variety of behaviors. Eur. Phys. J. E 23, 199–215. doi:10.1140/epje/i2006-10175-0.

Gran, K., Paola, C., 2001. Riparian vegetation controls on braided stream dynamics. Water Resources Research 37, 3275–3283.

Grant, G., 1997. Critical flow contrains flow hydraulics in mobile-bed streams: a new hypothesis. WRR 33, 349–358.

Hassan, W.N., Ribberink, J.S., 2005. Transport processes of uniform and mixed sands in oscillatory sheet flow. Coastal Engineering 52, 745–770. doi:http://dx.doi.org/10.1016/j.coastaleng.2005.06.002.

Hoyal, D., Sheets, B., 2009. Morphodynamic evolution of experimental cohesive deltas. J. of Geophys. Res. 114, F02009. doi:10.1029/2007JF000882.

Hughes, S., 1993. Physical models and laboratory techniques in coastal engineering. Advanced Series on Ocean Engineering, Vol. 7, World Scientific.

Iverson, R., Logan, M., LaHusen, R., Berti, M., 2010. The perfect debris flow? Aggregated results from 28 large-scale experiments. J. Geophys. Res. 115, F03005. doi:10.1029/2009JF001514.

Jin, D., Schumm, S., 1987. A new technique for modeling river morphology, in: Gardiner, V. (Ed.), International Geomorphology, Part I, Wiley, Chichester, UK. pp. 681–690.

Keulegan, G.H., 1938. Laws of turbulent flow in open channels. volume 21. Research Paper 1151, National Bureau of Standards.

Kleinhans, M.G., 2005a. Flow discharge and sediment transport models for estimating a minimum timescale of hydrological activity and channel and delta formation on Mars. J. of Geophysical Research 110, E12003. doi:10.1029/2005JE002521.

Kleinhans, M.G., 2005b. Phase diagrams of bed states in steady, unsteady, oscillatory and mixed flows, in: Van Rijn, L.C., Soulsby, R.L., Hoekstra, P., Davies, A. (Eds.), Sandpit project, Aqua Publications, Amsterdam, The Netherlands. pp. Q1–Q16.

Kleinhans, M.G., 2010. Sorting out river channel patterns. Progress in Physical Geography 34, 287–326. doi:10.1177/0309133310365300.

Kleinhans, M.G., Buskes, C., de Regt, H., 2005. Terra Incognita: Explanation and reduction in earth science. Int. Studies in the Philosophy of Science 19, 289–317. doi:10.1080/02698590500462356.

Kleinhans, M.G., van Dijk, W.M., van de Lageweg, W.I., Hoendervoogt, R., Markies, H., Schuurman, F., 2010a. From nature to lab: scaling self-formed meandering and braided rivers, in: Dittrich, Koll, Aberle, Geisenhainer (Eds.), Riverflow 2010, volume 2, Bundesanstalt fÃijr Wasserbau. pp. 1001–1010.

Kleinhans, M.G., van de Kasteele, H., Hauber, E., 2010b. Palaeoflow reconstruction from fan delta morphology on Mars. Earth and Planetary Science Letters 294, 378–392. doi:10.1016/j.epsl.2009.11.025.

Kleinhans, M.G., van den Berg, J.H., 2011. River channel and bar patterns explained and predicted by an empirical and a physics-based method. Earth Surf. Process. Landforms 36, 721–738. doi:10.1002/esp.2090.

Kleinhans, M.G., Van Rijn, L.C., 2002. Stochastic prediction of sediment transport in sand-gravel bed rivers. J. of Hydraulic Engineering 128, 412–425.

Kleinhans, M.G., van der Vegt, M., Terwisscha van Scheltinga, R., Baar, A., Markies, H., 2012. Turning the tide: experimental creation of tidal channel networks and ebb deltas. Netherlands J. of Geoscience 91, 311–323.

Koch, F., Flokstra, C., 1981. Bed level computations for curved alluvial channels. Proc. of the XIX Congress of the Int. Ass. for Hydr. Res., New Delhi, India 2, 357.

Kraal, E., van Dijk, M., Postma, G., Kleinhans, M.G., 2008. Martian stepped-delta formation by rapid water release. Nature 451, 973–976. doi:10.1038/nature06615.

Van de Lageweg, W.I., Van Dijk, W.M., Hoendervoogt, R., Kleinhans, M.G., 2010. Effects of riparian vegetation on experimental channel dynamics, in: Dittrich, Koll, Aberle, Geisenhainer (Eds.), Riverflow 2010, volume 2, Bundesanstalt fÃijr Wasserbau. pp. 1331–1338.

Lick, W., Gailani, J., 2004. Initiation of movement of quartz particles. J. of Hydraulic Engineering 130, 755–761.

Malverti, L., Lajeunesse, E., Métivier, F., 2008. Small is beautiful: Upscaling from microscale laminar to natural turbulent rivers. J. Geophys. Res. 113, F04004. doi:10.1029/2007JF000974.

Marra, W., Braat, L., Baar, A., Kleinhans, M.G., 2014. Valley formation by groundwater seepage, pressurized groundwater outbursts and crater-lake overflow in flume experiments with implications for Mars. Icarus doi:10.1016/j.icarus.

Marra, W.A., Kleinhans, M., Addink, E., 2013. Network concepts to describe channel importance and change in multichannel systems: test results for the jamuna river, bangladesh. Earth Surface Processes and Landforms doi:10.1002/esp.3482.

Metivier, F., Meunier, P., 2003. Input and output mass flux correlations in an experimental braided stream. Implications on the dynamics of bed load transport. J. of Hydrology 271, 22–38.

Meyer-Peter, E., Mueller, R., 1948. Formulas for bed-load transport, in: Proceedings 2nd meeting, Int. Ass. for Hydraulic Structures Res., Stockholm, Sweden. pp. 39–64.

Morgan, M., 2003. Experiments without material intervention: model experiments, virtual experiments, and virtually experiments. in: H. Radder (Ed.), The philosophy of scientific experimentation, University of Pittsburgh Press, Pittsburgh, USA. chapter 11. pp. 216–235.

Nagase, K., Sakaguchi, K., 1965. Alkaline hydrolysis of polyacrilamide. J. Polymer Sci. A3, 2475.

Oreskes, N., Shrader-Frechette, K., Belitz, K., 1994. Verification, validation and confirmation of numerical models in the earth sciences. Science 263, 641–642.

Paola, C., Borgman, L., 1991. Reconstructing random topography from preserved stratification. Sedimentology 38, 553–565.

Paola, C., Heller, P., Angevine, C., 1992. The large-scale dynamics of grain-size variation in alluvial basins. I: Theory. Basin Res. 4, 73–90.

Paola, C., Straub, K., Mohrig, D., Reinhardt, L., 2009. The "unreasonable effectiveness" of stratigraphic and geomorphic experiments. Earth-Science Reviews 97, 1–43. doi:10.1016/j.earscirev.2009.05.003.

Parker, G., 1978. Self-formed straight rivers with equilibrium banks and mobile bed. Part 2. The gravel river. J. Fluid Mech. 89, 127–146.

Parker, G., 2004. 1D Sediment Transport Morphodynamics with Applications to Rivers and Turbidity Currents. http://www.cee.uiuc.edu/people/parkerg/morphodynamics_e-book.htm.

Parker, G., Klingeman, P., 1982. On why gravel bed streams are paved. Water Resources Research 18, 1409–1423.

Peakall, J., Ashworth, P., Best, J., 1996. Physical modelling in fluvial geomorphology: principles, applications and unresolved issues, in: Rhoads, B., Thorn, C. (Eds.), The scientific nature of geomorphology, Wiley, Chichester, UK. pp. 221–253.

Peakall, J., Ashworth, P., Best, J., 2007. Meander-bend evolution, alluvial architecture, and the role of cohesion in sinuous river channels: a flume study. J. of Sedimentary Research 77, 197–212. doi:10.2110/jsr.2007.017.

Perona, P., Molnar, P., Crouzy, B., Perucca, E., Jiang, Z., McLelland, S., Wüthrich, D., Edmaier, K., Francis, R., Camporeale, C., Gurnell, A., 2012. Significance of the riparian vegetation dynamics on meandering river morphodynamics. Water Resources Research 43, W03430.

Postma, G., Cartigny, M., Kleverlaan, K., 2009. Structureless, coarse-tail graded Bouma Ta formed by internal hydraulic jump of the turbidity current? Sedimentary Geology 219, 1–6.

Powell, E., Kim, W., Muto, T., 2012. Varying discharge controls on timescales of autogenic storage and release processes in fluvio-deltaic environments: Tank experiments. J. Geophys. Res. 117, F02011. doi:10.1029/2011JF002097.

Reynolds, O., 1887. On certain laws relating to the regime of rivers and estuaries and on the possibility of experiments on a small scale. Br. Assoc. Rep. London, 555–562.

Rhoads, B., Miller, M., 1991. Impact of flow variability on the morphology of a low-energy meandering river. Earth Surf. Process. Landforms 16, 357–367. doi:10.1002/esp.3290160408.

Ribberink, J., Van der Sande, J., 1985. Aggradation in rivers due to overloading - analytical approaches. J. of Hydraulic Research 23, 273–283. doi:10.1080/00221688509499355.

Sambrook Smith, G., Best, J., Ashworth, P., Lane, S., Parker, N., Lunt, I., Thomas, R., Simpson, C., 2010. Can we distinguish flood frequency and magnitude in the sedimentological record of rivers? Geology 38, 579–582. doi:10.1130/G30861.1.

Schumm, S., Khan, H., 1972. Experimental study of channel patterns. Geol. Soc. of America. Bull. 83, 1755–1770.

Schumm, S., Mosley, M., Weaver, W., 1987. Experimental Fluvial Geomorphology. Wiley, New York, USA, 413 p.

Schuurman, F., Marra, W., Kleinhans, M.G., 2013. Physics-based modeling of large braided sand-bed rivers: bar pattern formation, dynamics and sensitivity. J. of Geophysical Research doi:10.1002/2013JF002896.

Seminara, G., Tubino, M., 1989. Alternate bars and meandering: free, forced and mixed interactions, in: Ikeda, S., Parker, G. (Eds.), River Meandering, American Geophysical Union, Washington D.C.. pp. 153–180.

Sheets, B.A., Hickson, T.A., Paola, C., 2002. Assembling the stratigraphic record: depositional patterns and time-scales in an experimental alluvial basin. Basin Research 14, 287–301.

Simon, A., Collinson, A., 2002. Quantifying the mechanical and hydrologic effects of riparian vegetation on streambank stability. Earth Surface Processes and Landforms 27, 527–546. doi:10.1002/esp.325.

Simon, A., Curini, A., Darby, S., Langendoen, E., 2000. Bank and near-bank processes in an incised channel. Geomorphology 35, 183–217.

Smith, C., 1998. Modeling high sinuosity meanders in a small flume. Geomorphology 25, 19–30.

Solari, L., Parker, G., 2000. The curious case of mobility reversal in sediment mixtures. J. of Hydraulic Engineering 126, 185–197.

Southard, J.B., Boguchwal, A.L., 1990. Bed configurations in steady unidirectional water flows. Part 2. Synthesis of flume data. J. of Sedimentary Petrology 60, 658–679.

Stefanon, L., Carniello, L., D'Alpaos, A., Lanzoni, S., 2010. Experimental analysis of tidal network growth and development. Continental Shelf Research 30, 950–962. doi:doi:10.1016/j.csr.2009.08.018.

Struiksma, N., 1986. Scale effects in the reproduction of the overall bed topography in river models. IAHR Symposium on Scale effects in modelling sediment transport phenomena, Toronto, Canada.

Struiksma, N., Klaassen, G., 1986. Experimental comparison of scaling with sand and bakelite as bed material. IAHR Symposium on Scale effects in modelling sediment transport phenomena, Toronto, Canada.

Struiksma, N., Olesen, K., Flokstra, C., De Vriend, H., 1985. Bed deformation in curved alluvial channels. J. of Hydraulic Research 23, 57–79.

Tal, M., Paola, C., 2007. Dynamic single-thread channels maintained by the interaction of flow and vegetation. Geology 35, 347–350. doi:10.1130/G23260A.1.

Tal, M., Paola, C., 2009. Effects of vegetation on channel morphodynamics: results and insights from laboratory experiments. Earth Surf. Proc. Landf. in press.

Tal, M., Paola, C., 2010. Effects of vegetation on channel morphodynamics: Results and insights from laboratory experiments. Earth Surface Processes and Landforms 35, 1014–1028. doi:10.1002/esp.1908.

Talmon, A., Struiksma, N., van Mierlo, M., 1995. Laboratory measurements of the direction of sediment transport on transverse alluvial-bed slopes. J. of Hydraulic Research 33, 495–517.

Tambroni, N., Bolla Pittaluga, M., Seminara, G., 2005. Laboratory observations of the morphodynamic evolution of tidal channels and tidal inlets. J. Geophys. Res. 110, F04009.

van de Lageweg, W., van Dijk, W., Kleinhans, M., 2013a. Channel belt architecture formed by an experimental meandering river. Sedimentology 60, 840–859. doi:10.1111/j.1365-3091.2012.01365.x.

van de Lageweg, W., van Dijk, W., Kleinhans, M., 2013b. Morphological and stratigraphical signature of floods in a braided gravel-bed river revealed from flume experiments. J. Sed. Res. 83, 1032–1045. doi:10.2110/jsr.2013.70.

van den Berg, J., 1995. Prediction of alluvial channel pattern of perennial rivers. Geomorphology 12, 259–279.

van den Berg, J., van Gelder, A., 1993. A new bedform stability diagram, with emphasis on the transition of ripples to plane bed in flows over fine sand and silt. International Association of Sedimentologists. volume 17. pp. 11–21.

van Dijk, M., Kleinhans, M.G., Postma, G., Kraal, E., 2012. Contrasting morphodynamics in alluvial fans and fan deltas: effect of the downstream boundary. Sedimentology 59, 2125–2145. doi:10.1111/j.1365-3091.2012.01337.x.

van Dijk, M., Postma, G., Kleinhans, M.G., 2009. Autogenic processes on experimental fan deltas. Sedimentology 56, 1569–1589. doi:10.1111/j.1365-3091.2008.01047.x.

Van Dijk, W.M., Teske, R., Van de Lageweg, W.I., Kleinhans, M.G., 2013a. Effects of vegetation distribution on experimental river channel dynamics. Water Resources Research 49, 7558–7574. doi:10.1002/2013WR013574.

Van Dijk, W.M., Van de Lageweg, W.I., Kleinhans, M.G., 2012. Experimental meandering river with chute cutoffs. Journal of Geophysical Research 117, F03023. doi:10.1029/2011JF002314.

Van Dijk, W.M., Van de Lageweg, W.I., Kleinhans, M.G., 2013b. Formation of a cohesive floodplain in a dynamic experimental meandering river. Earth Surface Processes and Landforms 38, 1550–1565. doi:10.1002/esp.3400.

van Rijn, L., 1984. Sediment transport, part I: bed load transport. J. of Hydraulic Engineering 110, 1431–1456.

Vollmer, S., Kleinhans, M.G., 2007. Predicting incipient motion including the effect of turbulent pressure fluctuations in the bed. Water Resources Research 43, W05410. doi:doi:10.1029/2006WR004919.

Vollmer, S., Kleinhans, M.G., 2008. Effects of particle exposure, near-bed velocity and pressure fluctuations on incipient motion of particle-size mixtures, in: Dohmen-Janssen, C., Hulscher, S. (Eds.), River, Coastal and Estuarine Morphodynamics 2007, Taylor and Francis/Balkema, London, UK. pp. 541–548.

Welber, M., Bertoldi, W., Tubino, M., 2013. Wood dispersal in braided streams: Results from physical modeling. Water Resources Research , n/a–n/adoi:10.1002/2013WR014046.

Wiberg, P., Smith, J., 1987. Calculations of the critical shear stress for motion of uniform and heterogeneous sediments. Water Resources Research 23, 1471–1480.

Wilcock, P., 1993. Critical shear stress of natural sediments. J. of Hydraulic Engineering 119, 491–505.

Wilcock, P., Crowe, J., 2003. Surface-based transport model for mixed-size sediment. J. of Hydraulic Engineering 129, 120–128. doi:10.1061/(ASCE)0733-9429(2003)129:2(120).

Wolman, M., Miller, J., 1960. Magnitude and frequency of forces in geomorphic processes. J. of Geology 68, 54–74.

Yalin, M., 1971. Theory of Hydraulic Models. Macmillan, London, UK.

Zanke, U.C.E., 2003. On the influence of turbulence on the initiation of sediment motion. International J. of Sediment Research 18, 1–15.